Building and Environment 136 (2018) 198–212

Contents lists available at ScienceDirect

Building and Environment

journal homepage: www.elsevier.com/locate/buildenv

Development of a nationally representative set of combined building energy and indoor air quality models for U.S. residences

Torkan Fazli, Brent Stephens*

Department of Civil, Architectural, and Environmental Engineering, Illinois Institute of Technology, 60616 Chicago, IL, USA

ARTICLE INFO

Keywords:
Indoor air pollution
EnergyPlus
Residential buildings
Building simulation
DALYs

ABSTRACT

Americans spend most of their time inside residences where they are exposed to a number of pollutants of both indoor and outdoor origin. Residential buildings also account for ~20% of the primary energy consumed in the U.S. To provide a tool for future investigations of interactions between energy use and indoor air quality (IAQ) in homes across the U.S. population, we developed a custom set of nationally representative building energy and IAQ mass balance models that predict annual energy use for space conditioning and indoor concentrations of a number of pollutants of both indoor and outdoor origin across the U.S. residential building stock. The residential energy and indoor air quality (REIAQ) model framework is built in Python and integrates between EnergyPlus and a dynamic mass balance model. REIAQ utilizes historical weather data to predict hourly energy consumption, air change rates, and HVAC system runtimes, which are coupled with historical outdoor pollutant concentration data and assumptions for indoor emission sources and other factors to predict hourly indoor pollutant concentrations. Modeled indoor pollutants include $PM_{2.5}$, UFPs, O_3, NO_2, and several volatile organic compounds (VOCs) and aldehydes. The REIAQ model set successfully predicted annual space conditioning energy consumption for the U.S. residential building stock within ~2% of historical data. Modeled indoor concentrations, infiltration factors for outdoor contaminants, and indoor/outdoor ratios of each pollutant all matched closely with observations from prior field studies. Population-weighted annual average indoor pollutant concentrations were also used to estimate the chronic health burden of residential indoor exposures.

1. Introduction

Americans spend most of their time inside their homes [1] where they are exposed to a number of airborne pollutants of both indoor and outdoor origin [2–5]. Both gases and particles of outdoor origin can infiltrate into homes with varying efficiencies [6–32]. Volatile organic compounds (VOCs) are emitted indoors from building materials [33,34], cleaning products [35,36], and personal care products [37]. Indoor sources of semi-volatile organic compounds (SVOCs) include plasticizers and flame retardants in building materials, as well as pesticides from both indoor and outdoor use [38]. Particles are generated indoors by smoking [9], cooking [39], burning incense and candles [40,41], operating office equipment and other appliances [42], and by resuspension from settled dust [43,44]. Moreover, reactions between oxidants such as ozone and reactive organic compounds in indoor air and adsorbed on surfaces form secondary gas- and particle-phase by-products [45–55].

Recent research has shown that concentrations of many pollutant concentrations inside residences often exceed chronic or acute health standards and are linked to adverse health outcomes ranging from sensory irritation to cancer. Logue et al. (2011) identified nine priority hazards in U.S. residences based on the magnitude of measured concentration data, the number of residences affected, and the prevalence of these pollutants at or above relevant health standards, including: acetaldehyde, acrolein, benzene, 1,3-butadiene, 1,4-dichlorobenzene, formaldehyde, naphthalene, nitrogen dioxide (NO_2), and $PM_{2.5}$ (i.e., the mass concentration of particles smaller than 2.5 μm in diameter) [56]. NO_2 and $PM_{2.5}$ are both regulated outdoors by the US EPA's National Ambient Air Quality Standards (NAAQS) and have both indoor and outdoor sources inside many homes. Two of these priority hazards, acetaldehyde and formaldehyde, are primarily emitted by indoor sources such as pressed-wood products and consumer products [57–59]. The cumulative chronic health impacts from inhalation of this wide array of indoor pollutants, excluding radon and secondhand smoke, have been estimated to result in between 400 and 1100 disability-adjusted life-years (DALYs) lost per 100,000 persons per year, representing an estimated 5–14% of the annual non-communicable, non-psychiatric disease burden in the U.S. [60]. Further, estimates of

* Corresponding author. Department of Civil, Architectural, and Environmental Engineering, Illinois Institute of Technology, 3201 S Dearborn Street, Alumni Hall Room 228, 60616 Chicago, IL, USA.
E-mail address: brent@iit.edu (B. Stephens).

https://doi.org/10.1016/j.buildenv.2018.03.047
Received 27 January 2018; Received in revised form 26 March 2018; Accepted 27 March 2018
Available online 28 March 2018
0360-1323/

Table 1
Summary of heating degree days (HDD), cooling degree days (CDD), and the number of dwellings and population represented by 19 cities across all ASHRAE climate zones and U.S. census divisions in the year 2000.

Cities	Census division	ASHRAE climate zone	HDD °C day	CDD °C day	# of Dwellings	U.S. Population in 2000
Atlanta, GA	South Atlantic	3A	1089	1169	3,686,721	14,857,749
Birmingham, AL	East South Central	3A	1077	1226	1,269,123	5,106,843
Boston, MA	New England	5A	2668	475	2,503,728	11,082,324
Buffalo, NY	Middle Atlantic	5A	3046	495	2,186,556	8,807,153
Chicago, IL	East North Central	5A	2752	776	10,689,222	39,330,037
Cincinnati, OH	East North Central	4A	2308	715	1,583,134	5,825,000
Corpus Christi, TX	West South Central	2A	254	2400	1,690,652	6,288,970
Dallas/Fort Worth, TX	West South Central	3A	914	1854	6,762,609	25,155,880
Denver, CO	Mountain	5B	2847	709	2,452,110	9,613,144
Los Angeles, CA	Pacific (South Pacific)	3B	722	323	7,788,014	32,013,228
Miami, FL	South Atlantic	1A	66	2321	3,905,099	15,737,825
Minneapolis, MN	West North Central	6A	3405	647	2,125,685	7,945,186
Nashville, TN	East South Central	4A	1555	1103	2,961,287	11,915,967
New York, NY	Middle Atlantic	4A	2259	652	7,662,797	30,864,708
Phoenix, AZ	Mountain	2B	372	2889	2,183,259	8,559,151
Seattle, WA	Pacific	4C	2551	91	3,165,592	13,012,409
St. Louis, MO	West North Central	4A	1940	1263	3,021,253	11,292,553
Washington, DC	South Atlantic	4A	2133	792	5,253,899	21,173,586
Worcester, MA	New England	4A	3137	360	641,659	2,840,193
Total					**71,532,391**	**281,421,906**

cumulative lifetime cancer risks from exposure to a combination of several hazardous indoor air pollutants in homes typically range from 1 to 10 excess cases per 10,000 people [61–63].

Residential buildings also account for approximately 20% of the primary energy consumed in the U.S. annually [64]. Over 60% of existing residential buildings and approximately 90% of newly constructed residences in the U.S. use central forced-air distribution systems for air-conditioning purposes [65], and almost 50% of primary energy used in U.S. residences is for space heating and cooling [66]. Further, many source and removal mechanisms of indoor pollutants are closely tied to energy consumption, and changes made to improve indoor air quality can impact energy consumption. For example, high outdoor air infiltration rates lead to higher energy consumption and can also be a major source of pollutants in homes, but can also serve to dilute concentrations of indoor-generated pollutants [67]. As air infiltration rates continue to decrease with more widespread energy-efficient building construction practices [68–70], new tools are needed to understand how concentrations of outdoor-infiltrated and indoor-generated pollutants might change as the building stock changes over time. As another example, central heating, ventilation, and air-conditioning (HVAC) filters are often relied upon to remove indoor pollutants, but their effectiveness depends on both filter efficiency and system operational characteristics [71–73]. Additionally, the energy consequences of improved filtration and mechanical ventilation are also intricately linked to system design and operational characteristics [74–78].

Because field measurements of energy use and indoor air quality in large numbers of homes can be prohibitively expensive and time consuming, accurate and robust simulation tools for predicting energy use and indoor pollutant concentrations that aggregate across large numbers of individual buildings are needed to investigate interactions between energy use and indoor air quality (IAQ) across the population. To aid in this effort, we have developed a nationally representative residential energy and IAQ (REIAQ) model set that can be used to predict energy use for space conditioning and indoor concentrations of a number of pollutants of both indoor and outdoor origin across the U.S. residential building stock. The goal is to provide a workflow that integrates freely available simulation software packages to perform population-wide impact analyses that can ultimately inform building designers, standards organizations, and policy makers of the complex interactions between energy and indoor air quality in U.S. residences.

2. Methods

The residential energy and IAQ (REIAQ) model framework combines hourly energy simulations using BEopt Version 2.2.0 and EnergyPlus Version 8.1.0 with a custom hourly mass balance model for dynamic indoor pollutant simulations. The model process is an indirect co-simulation process in which energy, airflow, and contaminant mass balance equations are not solved as an integrated set of equations but rather are solved sequentially as described below. The model framework is built in Python 2.7 to automate the majority of the simulation process. The model process involves the following sequential steps: (1) manually constructing a minimal number of typical home geometries required in BEopt, (2) modifying those base home geometries to include region-specific details on envelope construction, HVAC characteristics, and other characteristics for use in energy simulations, (3) running hourly energy simulations in EnergyPlus, (4) passing hourly energy simulation outputs such as modeled hourly air change rates (ACRs) and central HVAC system runtimes to a transient indoor air mass balance model to simulate hourly concentrations of several priority pollutants of both indoor and outdoor origin, and (5) aggregating hourly model results over the course of the model year and applying population-weighting factors to generate nationally representative average concentrations of each pollutant and an aggregate estimate of the total annual heating and cooling energy consumption in U.S. residences. Resulting population-average indoor pollutant concentrations are also used to generate estimates of the population-wide chronic health impacts associated with residential indoor exposures following a recently developed methodology that uses a disability-adjusted life-years (DALYs) approach. Each of these steps is described in more detail in the following sections.

2.1. Building the nationally representative set of home models

The model set is built upon the housing characteristics and model geometries detailed in Persily et al. (2010) [79] and Persily et al. (2006) [80], which described the development of a set of models of 209 dwellings that represent approximately 80% of all U.S. residences as of approximately the year 2000. We used the same allocation of the dwellings as the NIST model set, with homes located across 19 of the most populous cities in the U.S. that cover all ASHRAE climate zones and all 9 U.S. census divisions (Table 1).

The set of 209 dwellings are grouped into four categories: detached,

attached, manufactured homes, and apartments. The primary characteristics used to distinguish the baseline collection of residences include floor area, year built, number of floors, foundation type, whether or not they have a forced air distribution system, and the presence or lack of an attached garage (SI Appendix A). These models are considered current as of approximately 2000 and no changes have been made at this point to include newer homes built since then, although updates to the model set are planned for future work. While the NIST models were originally built for multi-zone indoor airflow modeling in CONTAM [81], we transcribed the base model set to BEopt models for energy simulation with EnergyPlus and also used their base characteristics to construct single-zone well-mixed reactor models for indoor pollutant simulations. We chose to build our own single-zone model for several reasons, including (i) model development began prior to the recent development of software to couple CONTAM and EnergyPlus [82] and (ii) we did not necessarily require multi-zone modeling capabilities for this type of aggregate population-level analysis [83,84].

To convert the 209 dwellings into BEopt models, we first identified the minimum number of identical home geometries that were used in the NIST model set. A total of 114 minimal base model home geometries were first constructed manually in BEopt, which generated 114 XML input files that each provide a complete description of a single building with an element for every input found in the BEopt interface [85]. To increase this number to be consistent with the same 209 dwelling models used in the NIST data set, we made adjustments to the 114 BEopt XML files of base model home geometries, which included selecting various foundation types (e.g., concrete slab, crawl space, or basement as dictated by the most typical construction characteristics in climate zone), selecting attached or detached garages, and selecting detached or attached home construction. We manually assigned these characteristics following the NIST model set directly.

Next, multiple versions of the 209 BEopt XML files for the base model home geometries were created using an automated scripting process to incorporate other important home characteristics that were assumed to vary by climate zone and year of construction, with each of the 19 cities having a different proportion of homes assigned by vintage, types of heating and cooling system, building envelope insulation levels, and thermostat settings. Two residential building databases, including the U.S. Census Bureau's American Housing Survey (1999) [86] and the U.S. Department of Energy's Residential Energy Consumption Survey (1997) [87], were used to inform the assignment of typical home characteristics to each multiple of the base model home geometries. The assignment of these more detailed home characteristics resulted in a total of 3971 home models in the form of BEopt XML files (i.e., 209 homes × 19 cities = 3971 home models). These more detailed home characteristics are described in the following subsections.

2.1.1. Envelope airtightness

Building envelope airtightness is well known to vary by the year of the construction of homes [69,70,88]. The original NIST model set assigned a level of airtightness to each home model using specific values of Normalized Leakage (NL) areas that varied according to both floor area and vintage. However, by default, BEopt uses only the air changes per hour at an indoor-outdoor pressure difference of 50 Pa (i.e., ACH_{50}) to define the envelope airtightness of a home model. Therefore, we converted the NL values assigned in the NIST model set to ACH_{50} values using typical pressure and flow relationships from fan pressurization tests, as shown in Equations (1)–(4) [67,69,89] and in Table 2.

$$Q = ELA\sqrt{\frac{2P_r}{\rho}}\left(\frac{\Delta P}{P_r}\right)^n \tag{1}$$

$$NL = 1000\,\frac{ELA}{A_f}\left(\frac{H}{2.5m}\right)^{0.3} \tag{2}$$

Table 2
Exterior enclosure leakage values for the model homes based on vintage and floor area.

Year built	Floor Area < 148.6 m^2		Floor Area > 148.6 m^2	
	NL (−)	ACH_{50} (1/hr)	NL (−)	ACH_{50} (1/hr)
Before 1940	1.29	27	0.58	12
1940–1969	1.03	21	0.49	10
1970–1989	0.65	13	0.36	7
1990 and newer	0.31	7	0.24	5

$$ACH_{50} = \frac{Q_{50}}{V} \tag{3}$$

$$ACH_{50} = NL \times \frac{66}{H^{1.3}} \tag{4}$$

where Q = airflow rate $\left(\frac{m^3}{s}\right)$, ELA = effective leakage area (m^2), P_r = reference pressure (Pa), ρ = air density $\left(\frac{kg}{m^3}\right)$, ΔP = indoor–outdoor pressure difference (Pa), n = pressure exponent (−), A_f = floor area (m^2), H = height (m), Q_{50} = airflow rate at a pressure difference of 50 Pa (m^3/h), and V = volume of the building (m^3). We assumed $n = \frac{2}{3}$ and $\rho = 1.2\frac{kg}{m^3}$ for typical conditions to estimate ACH_{50} directly from NL using Equation (4).

2.1.2. Types of heating and cooling systems

Each of the 3971 home models was then assigned the most common type of heating and cooling equipment for each home vintage in each climate zone and U.S. census division based on information provided in RECS and in the NIST data set (SI Appendix A). Other less common types of heating and cooling equipment were not modeled to keep the number of simulations to a manageable amount. In total, four types of heating equipment and two types of cooling equipment were modeled. Homes with central forced-air distribution systems were modeled either with a gas or electric furnace for heating and a central air conditioner for cooling or with air-source heat pumps that provided both heating and cooling in one integrated system. Homes without central forced-air distribution systems were modeled with either a gas or oil boiler or with electric baseboard heating and with only room air conditioners for cooling. For homes that had central forced-air distribution systems located in unconditioned spaces, the systems were assumed to have 10% duct leakage to the exterior. All other home models were assumed to have 0% duct leakage to the exterior.

We also made several assumptions for the nominal efficiency of each heating and cooling system type in each home based on vintage using a combination of default values from BEopt and a previously published report on building system performance characteristics for existing homes [90]. The distribution of each type of heating and cooling system and their assumed efficiencies and fuel sources, varying by vintage, is shown in Table 3.

2.1.3. Thermal performance of the building enclosure

Building envelope thermal performance also varied based on the year of construction and the location of each of the 3971 home models. While these characteristics were not included in the original NIST model set, we made assumptions for the most common envelope thermal performance characteristics. Exterior wall materials, wall, roof, and floor insulation levels, and window areas, U-values, and solar heat gain coefficients (SHGC) were assigned for each vintage and climate zone following various surveys of U.S. residences built before 1990 [91–93] and following the International Energy Conservation Code for homes built after 1990 [94]. The latter assumption may introduce some uncertainty in newer home vintages because actual construction and performance can vary from code minimum requirements. A full list of home characteristics for each construction year and city is provided in

Table 3
Type and efficiency of heating and cooling equipment assumed for each home vintage.

HVAC systems		HVAC fuel	Year built			
			< 1940	1940–1969	1970–1989	> 1990
Heating equipment	Furnace	Gas	78% AFUE	80% AFUE	90% AFUE	92.5% AFUE
		Electricity	100% AFUE	100% AFUE	100% AFUE	100% AFUE
	Heat pump	Electricity	COP 1.8 (6 HSPF)	COP 1.8 (6 HSPF)	COP 1.9 (6.6 HSPF)	COP 2.1 (7.1 HSPF)
	Boiler	Gas	55% AFUE	60% AFUE	72% AFUE	80% AFUE
		Oil	55% AFUE	60% AFUE	72% AFUE	80% AFUE
	Baseboard	Electricity	100% efficiency	100% efficiency	100% efficiency	100% efficiency
Cooling equipment	Central air conditioner	Electricity	COP 1.9 (SEER 6.5)	COP 2.1 (SEER 7.3)	COP 2.7 (SEER 10)	COP 3.3 (SEER 13)
	Heat pump	Electricity	COP 1.9 (SEER 6.5)	COP 1.9 (SEER 6.5)	COP 2.3 (SEER 8)	COP 2.7 (SEER 10)
	Room conditioner	Electricity	COP 1.9 (EER 6.5)	COP 1.9 (EER 6.5)	COP 2.2 (EER 7.5)	COP 2.5 (EER 8.5)

the SI (Appendix B). Generally, older vintage homes were assumed to have minimal building envelope insulation and newer vintage homes were assumed to have greater levels of envelope insulation.

2.1.4. Thermostat set points

Heating and cooling thermostat set points were assumed to vary by climate zone using data from the 2009 U.S. DOE RECS [95]. Table 4 shows the average thermostat temperature set points for both heating and cooling seasons in different U.S. climate zones provided in RECS. There were no values provided in the Marine climate zones, so we assumed that homes in these regions had the same thermostat set points as Cold regions because they had similar numbers of cooling degree days.

2.2. Energy simulation procedures

EnergyPlus was used to simulate hourly heating and cooling energy consumption, HVAC system runtimes, and air change rates (ACRs) through infiltration, natural ventilation, and mechanical ventilation separately for each model scenario. Once the 3971 BEopt XML input files were generated and edited for specific characteristics based on vintage and climate zone, EnergyPlus input files (IDF files) were generated for each unique home model. Heating and cooling equipment was first auto-sized for each home with a central heating and/or cooling system using EnergyPlus, but because the auto-sizing procedure results in non-standardized equipment capacities that would yield inaccurate system runtimes, we used common commercially available incremental air-conditioner, furnace, and heat pump capacities to increase the auto-sized capacities of each piece of equipment to a more realistic size [76]. Increments of 1.76 kW and 3.5 kW were used for cooling and heating equipment capacities, respectively.

For each home model with a central forced air heating and/or cooling system, we made the following assumptions. The air handling unit was assumed to operate with a constant airflow rate of 193 m^3/h per kW of cooling capacity in both heating and cooling seasons [74,96]. El Orch et al. (2014) estimated that more than 55% of U.S. residences use MERV 6 or lower HVAC filters [24]; thus, we assumed that all central air handling units had MERV 6 particle filters installed. This assumption underrepresents the use of both lower and higher efficiency filters, but because there are no known data sets of filter use by region and/or home vintage, this serves as a reasonable assumption for a typical home in each location.

To account for the impact of filter and system pressure drop on fan pressure rise and fan efficiency, we modified the default assumptions for fan pressure rise from BEopt because field measurements consistently demonstrate that fan pressure is higher than what most standards and simulation programs assume [76,97,98]. In one of the larger field investigations of fan pressure in residences of which we are aware, Proctor (2012) reported an average total external static pressure of ~220 Pa in residential air-conditioning systems in 80 homes in California [99]. Since most residential air handling units in the U.S. as of 2000 used permanent split capacitor (PSC) fan motors [100], all modeled air handling units were assumed to have PSC motors. The fan efficiency for all homes with a fan pressure rise of 220 Pa was estimated to be 26% based on virtual models of generally representative PSC blowers [101].

We assumed that there were no dedicated whole-house mechanical ventilation systems in any of the home models. This is a conservative estimate that is surprisingly accurate at scale for some regions but less accurate for others, but we consider this a reasonably realistic assumption for the majority of the building stock as of approximately the year 2000. For spot ventilation systems, a nationwide survey of households in 1985 reported that only half of U.S. residents surveyed used vented range hoods and about 40% of residents with vented range hoods used their fan while preparing dinner meals [102]. In a more recent survey of California households, Klug et al. (2012) reported a similar percentage (42.4%) of range hood usage during dinner preparation [103]. To reasonably approximate the range hood use and usage survey data, homes built before 1970 were assumed to not have a kitchen range hood and homes built after 1970 were assumed to have a vented kitchen range hood with an airflow rate of 170 $\frac{m^3}{hr}$. To approximate range hood use by those households that have range hoods (i.e., ~40%), the kitchen range hood was assumed to operate three days per week for 1 h during dinner preparation (i.e., 6:00 p.m.–7:00 p.m.). We are not aware of nationwide surveys of bathroom exhaust fan existence or usage, so we used the default assumptions for bathroom exhaust fans

Table 4
Assumptions for heating and cooling thermostat set points by climate zone based on data from RECS [95].

Climate zone	Cities	Heating set point (°C)	Cooling set point (°C)
Hot-dry/mixed-dry	Los Angeles, Phoenix	19.6	24.5
Hot-humid	Atlanta, Corpus Christi, Dallas, Miami	20.5	24.3
Mixed-humid	Birmingham, Cincinnati, Nashville, New York, St. Louis, Washington	19.7	22.0
Very cold/cold	Boston, Buffalo, Chicago, Denver, Minneapolis, Seattle, Worcester	18.6	23.0

in BEopt of 1 h per day (i.e., 7:00 a.m.–8:00 a.m.) 7 days per week with an airflow rate of 85 $\frac{m^3}{hr}$ for the two newer home vintages. The two oldest vintages were assumed not to have exhaust fans. The assumptions for kitchen and bathroom exhaust airflow rates both reflect common nominal values based on ventilation standards (e.g., ASHRAE Standard 62.2), but measured airflow rates in real residences are often lower than nominal values. However, we are not aware of robust published data sets documenting actual versus nominal performance of exhaust fans and thus have assumed these nominal values for simplicity.

The natural ventilation (i.e., window opening) schedule was assumed to vary based on the presence of central forced-air heating and cooling systems in the home models following default assumptions in BEopt. Homes with central forced-air distribution systems were assumed to allow natural ventilation 3 days per week (Mondays, Wednesdays, and Fridays) to reflect windows being opened occasionally. Homes without central forced-air heating and cooling systems were assumed to allow natural ventilation 7 days a week. Default assumptions for daily window opening in BEopt are based on the 2014 Building America House Simulation Protocols [104]. Windows were assumed to be opened only when the outdoor air humidity ratio was less than 0.0115 kg_w/kg_{da} and the outdoor air relative humidity was less than 70%. Windows were assumed to be closed when the indoor air temperature dropped 0.5 °C below the heating or cooling set point or if the cooling load of outdoor airflow could not maintain the cooling set point. BEopt generates a program in EnergyPlus that combines assumptions for window opening schedules and window opening areas with meteorological conditions to estimate ventilation airflows through openings following the Sherman and Grimsrud model [67,105]. It is worth noting that this model was developed to predict infiltration airflows and has not, to our knowledge, been validated for predicting natural ventilation flows.

Because the intent of these simulations is to merge energy and IAQ mass balance modeling and the IAQ modeling involves culling hourly outdoor pollutant data for each city, we chose to conduct all modeling for a single actual meteorological year (AMY) rather than using typical meteorological year (TMY) weather files. While there are some disadvantages of using only single year weather files (e.g., they are not representative of other years), the advantages of syncing weather and outdoor pollutant data files as inputs were crucial for this modeling effort [73]. Therefore, we used AMY data from the year 2012, which was the most recent year for which hourly outdoor pollutant data were also available (as described in the next section), for inputs to the energy simulations. These historical weather files are purchased from White Box Technologies for all 19 cities [106]. Simulation time steps were set to 6 per hour in EnergyPlus for all energy simulations.

2.3. Application of the model set for predicting indoor pollutant concentrations

After performing energy simulations for each of the 3971 model home scenarios, dynamic indoor mass balance models were used to estimate hourly concentrations of a number of pollutants of both indoor and outdoor origin that have been previously identified as being of most concern to chronic health impacts across the U.S. residential building stock. Outdoor-generated pollutants included regulated pollutants that have well known associations with adverse health effects ($PM_{2.5}$, O_3, NO_2, and UFPs), three of which are also identified as priority pollutants in Logue et al. (2012) [60]. Indoor-generated pollutants included eight priority chronic health hazards identified in Logue et al. (2011) [5], including acetaldehyde, acrolein, benzene, 1,3-butadiene, 1,4-dichlorobenzene, and formaldehyde, as well as indoor sources of three of the outdoor pollutants: NO_2, $PM_{2.5}$, and UFPs. The mass balance models utilized several EnergyPlus outputs as inputs and we made several assumptions for typical indoor emission rates and other factors to reasonably reflect typical homes in the U.S.

2.3.1. Single-zone mass balance model

A discrete time-varying mass balance model for a single well-mixed zone was used to estimate the hourly concentrations of both indoor and outdoor generated pollutants in each home model. Hourly inputs were interpolated to 1-min intervals to improve model stability, and then 1-min mass balance model outputs were averaged on an hourly basis. The indoor concentration at the initial time step (i.e., midnight on January 1) was assumed to be the same as the steady state concentration for that initial time period. Indoor pollutant concentrations at each time step (t_n) were then estimated using Equation (5).

$$C_{in}(t_n) = C_{in}(t_{n-1}) + \Delta t \left[(P\lambda_{inf}(t_{n-1}) + \lambda_{nat}(t_{n-1}))C_{out}(t_{n-1}) + \frac{E(t_{n-1})}{V} - (\lambda_{inf}(t_{n-1}) + \lambda_{nat}(t_{n-1}))C_{in}(t_{n-1}) - \frac{Q_{exhaust}(t_{n-1})}{V}C_{in}(t_{n-1}) - \beta C_{in}(t_{n-1}) - f_{filt}(t_{n-1})\frac{\eta_{filt}Q_{filt}(t_{n-1})}{V}C_{in}(t_{n-1}) - kC_{terp}C_{in}(t_{n-1}) \right] \quad (5)$$

where C_{in} = the indoor concentration of any airborne pollutant (# m^{-3} or $\mu g\ m^{-3}$ for particles; ppb by volume or $\mu g\ m^{-3}$ for gases), P = the penetration factor of the building envelope for a particular pollutant (dimensionless, ranging from 0 to 1), λ_{inf} = the air change rate due to infiltration alone (h^{-1}), C_{out} = the outdoor pollutant concentration (# m^{-3} or $\mu g\ m^{-3}$ for particles; ppb by volume or $\mu g\ m^{-3}$ for gases), E = the whole-house indoor emission rate of a pollutant ($\mu g\ h^{-1}$ or # h^{-1}), V = the volume of the home (m^3), $Q_{exhaust}$ = the airflow rate of any mechanical exhaust ventilation system ($m^3\ h^{-1}$), β = the first-order indoor loss rate of the pollutant by deposition to surfaces and/or surface reactions (h^{-1}), η_{filt} = the pollutant removal efficiency of a filter installed the HVAC system if applicable (dimensionless, ranging from 0 to 1), Q_{filt} = the airflow rate through the central HVAC filter if applicable ($m^3\ h^{-1}$), f_{filt} = the fractional runtime of the HVAC system if applicable (dimensionless, ranging from 0 to 1), k = the bimolecular reaction rate constant between two gas-phase compounds ($m^3\ \mu g^{-1}\ h^{-1}$ or $ppb^{-1}\ h^{-1}$), C_{terp} = the concentration of a reactant ($\mu g\ m^{-3}$ or ppb), t_n is the current time step (h), and t_{n-1} is the previous time step (h). Values for each model input were culled from the literature as described below.

2.3.2. Outdoor pollutant data

Hourly outdoor pollutant data for $PM_{2.5}$, NO_2, and O_3 in each location were culled from the U.S. EPA Air Quality System (AQS) online repository for each of the 19 representative model locations for the year 2012 [107]. Data were visually inspected for missing values and, when there were gaps in the hourly data, hourly data from the next closest monitoring station were prioritized. If small gaps still remained and the number of missing data resulted in less than 95% of the total expected number of hourly data points, then linear interpolation was used to estimate any missing observations.

Outdoor UFP concentrations are not consistently measured in the U.S.; therefore, we made rough estimates of hourly outdoor UFP concentration data based on associations with NO_x concentrations using correlations reported by Azimi et al. [73]. It should be noted that absolute outdoor UFP concentration values are considered very approximate with high uncertainty using this method, although relative indoor-outdoor UFP concentrations ratios are more reliable. UFP concentrations (both indoors and outdoors) are not considered on a size-resolved basis at this point in time for model simplicity. Annual mean concentrations of ambient $PM_{2.5}$, O_3, NO_2, and UFPs (based on an assumed association with NO_x) for the 19 cities used herein are shown in Fig. 2. A detailed summary of the ambient air quality monitoring stations used for outdoor $PM_{2.5}$, O_3, NO_2, and NO_x is shown in the SI

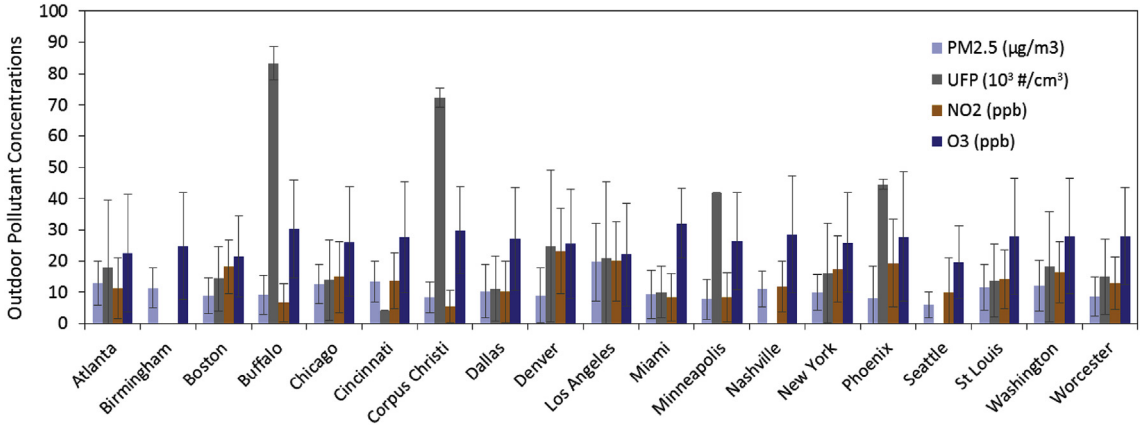

Fig. 1. Annual averages and standard deviations of hourly outdoor concentrations of $PM_{2.5}$, O_3, NO_2, and estimates of UFPs in the 19 cities used in the model set.

(Appendix C). Annual averages of hourly pollutant concentrations used in the model set are shown in Fig. 1.

Ambient concentrations of volatile organic compounds (VOCs) and aldehydes were assumed to be constant throughout the year, as hourly data are not widely available for these compounds. The geometric mean ambient concentrations from 48-h air samples collected in about 300 homes in the Relationships of Indoor, Outdoor, and Personal Air (RIOPA) study were used as these constant ambient concentrations [108], including 3.9, 2.3, 0.21, 0.1, 0.53, and 0.39 ppb for formaldehyde, acetaldehyde, acrolein, 1,3-butadiene, benzene, and 1,4-dichlorobenzene, respectively.

2.3.3. Indoor pollutant emission rates

For all indoor emission sources we used 'typical' emission rates and schedules, but to limit computation times we did not consider distributions of these parameters. Our intent was to provide reasonable estimates for typical homes across the U.S., and we believe that these assumptions reasonably reflect common emission sources even though source strengths and activity patterns will vary day-by-day and home-by-home [109]. Geometric mean whole-house emission rates for VOCs and aldehydes were taken from recent estimates based on the Relationships of Indoor, Outdoor, and Personal Air (RIOPA) database made in Waring (2014) [51]. Constant volume-normalized emission rates (i.e., E/V) for formaldehyde, acetaldehyde, acrolein, 1,3-butadiene, benzene and 1,4-dichlorobenzene were assumed to be 9.6, 4.0, 0.21, 0.15, 0.35, and 0.14 $\frac{ppb}{hr}$, respectively. Although chamber studies have shown that VOC and aldehyde emission rates from individual building materials can vary drastically with temperature and relative humidity [110,111], we are not aware of any studies linking these parameters to whole-house emission rates, which are required for our model inputs. Therefore, correlations between gas-phase emission rates and indoor environmental conditions are not included in the model in its current form.

Transient $PM_{2.5}$, NO_2, and UFP emission rates were assumed to follow scripted human activity patterns with typical source-strengths for the most common sources found in the literature. $PM_{2.5}$, UFP, and NO_2 emissions were assumed to be generated only from cooking, which was assumed to occur 1 h per day, every day, in the evening (6:00 p.m.–7:00 p.m.). We assumed that the $PM_{2.5}$ emission rate from cooking sources was 38.4 $\frac{mg}{hr}$, which was the median value from two of the most comprehensive studies of which we are aware that measured $PM_{2.5}$ emission rates from various cooking activities including frying, grilling, toasting, and microwaving various types of foods, with various types of cooking oils, and using both gas and electric stoves with both minimum and maximum power [112,113]. Furthermore, for gas stoves, which account for ~25% of the 209 baseline homes, UFP and NO_2 emission rates were assumed to be 1.13×10^{14} $\frac{\#}{hr}$ [4] and 123 $\frac{mg}{hr}$ [114,115], respectively, for each cooking event. The assumed NO_2 emission rate is the median value from two experimental studies that measured the NO_2 emission rate for various gas ranges, flame types, firing rates [115] and also variations in emission rates by age of gas stove [110]. For electric stoves, which account for ~75% of the 209 baseline homes, the UFP emission rate was assumed to be 7.5×10^{13} $\frac{\#}{hr}$ for each cooking event [4] (electric stoves were assumed to have no NO_2 emissions). For cooking events in homes modeled with vented kitchen range hoods, we assumed a pollutant capture efficiency of 40%, which was approximately the mean value reported in a recent study of range hoods used in U.S. residences [116]. A capture efficiency of 40% means that the emission rate for pollutants generated by cooking was simply reduced by 40% in the models when a range hood was operating.

2.3.4. Other pollutant source and loss mechanisms

Other pollutant source and loss mechanisms used in the mass balance in Equation (5) include building envelope penetration factors, indoor deposition loss rate coefficients, HVAC filter removal efficiencies (if applicable), and reaction rate constants for oxidation reactions between ozone and reactive organic gases (ROGs). Typical values for each of these parameters were culled from the literature. Again for simplicity and to minimize computation time, these inputs were kept constant in all home scenarios.

Envelope penetration factors (i.e., the fraction of contaminant in ambient air that passes through the building shell) during periods of infiltration only (i.e., with doors and windows closed) were assumed as follows. $PM_{2.5}$ penetration factors for all homes were assumed to be 0.82, which was calculated by mapping size-resolved particle penetration factor data from two previous studies of penetration factors in homes relying on infiltration alone [11,29] to size-resolved distributions of outdoor $PM_{2.5}$ concentrations for each size bin in a study by Logue et al. 2015 [83] (see SI Appendix D for more details). Envelope penetration factors for total UFPs (i.e., non-size-resolved) were assumed to be 0.47 based on the average reported in a recent study of 19 homes in Austin, Texas [19]. Ozone penetration factors were assumed to be 0.79 based on recent measurements in 8 homes in Austin, Texas [20]. Finally, NO_2 penetration factors were assumed to be 1.0 based on assumptions used in another recent modeling study [117]. Envelope penetration factors for each pollutant during periods of natural ventilation (i.e., with windows open) were assumed to be 1.0 for simplicity, although there is some evidence in the literature that this depends on how many windows open and how wide they are open [118]. There is also some evidence in the literature that envelope penetration factors for some pollutants may vary with home vintage [11,19,20], but there is not a large enough data set to make a robust association at this time. All VOCs and aldehydes with outdoor sources were assumed to have penetration factors of 1 at all times.

The indoor deposition rate for $PM_{2.5}$ was calculated in a similar manner as penetration factors (SI Appendix D). $PM_{2.5}$ deposition rates

were estimated to be 0.30 h^{-1} based on size-resolved deposition rate data reported in Logue et al. (2015) [83], which used a combination of data from Thatcher et al. (2003) and Long et al. (2001), in conjunction with data for typical indoor particle size distributions as reported in Abt et al. (2000) [119]. UFP deposition rates were assumed to be 0.70 h^{-1} based on a study of 45 non-smoking homes in Canada [120]. Deposition loss rate coefficients for O_3 were assumed to be the mean value of 2.8 h^{-1} from a study of homes in Southern California [121] and NO_2 deposition loss rate coefficients were assumed to be the mean value of 0.34 h^{-1} from a study of homes in Northern California [122]. All VOCs and aldehydes were assumed to have negligible indoor deposition loss rates and filtration efficiencies at all times, and sorption dynamics were also ignored for simplicity. Each of these values was assumed to be valid for times when windows remained closed, while each deposition loss rate coefficient was adjusted by a simple multiplier during times when windows were assumed to be open. We used a multiplier of 1.23 for these time periods, which was estimated in El Orch et al. based on a review of the relatively scarce literature on the impact of natural ventilation on indoor pollutant deposition rates [24].

As mentioned in Section 2.2, all homes with central HVAC systems were assumed to have a MERV 6 particle filter installed. We assumed a constant $PM_{2.5}$ and total UFP removal efficiency for MERV 6 filters of 8% and 8%, respectively, which we estimated by matching size-resolved removal efficiency data for MERV 6 filters reported in Hecker and Hofacre (2008) [123] to typical indoor particle size distributions reported by Abt et al. (2000) [119] (SI Appendix D). We assumed that HVAC filters had negligible removal efficiency for O_3, NO_2, and all VOCs and aldehydes.

Last, to account for basic gas-phase oxidation chemistry as an additional ozone removal mechanism and secondary organic aerosol (SOA) byproduct formation mechanism, we assumed typical values for reaction rate constants and indoor reactant concentrations for reactions between O_3 and the dominant reactive organic gases (ROGs: e.g., terpenes) that react with O_3 in homes: d-limonene and α-pinene. The concentration of these two reactants were modeled using the following mass balance equation:

$$C_{terp}(t_n) = C_{terp}(t_{n-1}) + \Delta t \left[(\lambda_{inf}(t_{n-1}) + \lambda_{nat}(t_{n-1}))C_{terp,out} + \frac{E_{terp}}{V} - (\lambda_{inf}(t_{n-1}) + \lambda_{nat}(t_{n-1}))C_{terp}(t_{n-1}) \right] \quad (6)$$

Outdoor concentrations and indoor emission rates of ROGs were assumed to be constant values taken from Waring 2014 [51]: $C_{terp,out}$ = 0.23 and 0.057 ppb and $\frac{E_{terp}}{V}$ = 1.5 and 0.23 $ppb\ h^{-1}$ for d-limonene and α-pinene, respectively. For the SOA formation model, the following mass balance equation was used:

$$C_{SOA}(t_n) = C_{SOA}(t_{n-1}) + \Delta t \left[\left(\sum_{terp} Y_{terp}(t_{n-1}) C_{terp}(t_{n-1}) k_{terp} \Gamma_{terp} \right) C_{O_3}(t_{n-1}) - \left(\lambda_{inf}(t_{n-1}) + \lambda_{nat}(t_{n-1}) + f_{filt}(t_{n-1}) \frac{\eta_{filt} Q_{filt}(t_{n-1})}{V} + \beta_{SOA} \right) C_{SOA}(t_{n-1}) \right] \quad (7)$$

where C_{SOA} = the indoor secondary organic aerosol mass concentration ($\mu g\ m^{-3}$), Y_{terp} = SOA mass formation yield for the ozonolysis of indoor terpenoids, k_{terp} = the reaction rate constant between ozone and terpenoids ($ppb^{-1}h^{-1}$), which were assumed to be 1.9×10^{-2} $ppb^{-1}\,h^{-1}$ and 7.9×10^{-3} $ppb^{-1}\,h^{-1}$ for d-limonene and α-pinene, respectively [51], C_{terp} = the concentration of a reactant (ppb), and Γ_{terp} = conversion factor to change between ppb and $\mu g\ m^{-3}$, and β_{SOA} = the first-order indoor loss rate of the pollutant by deposition to surfaces and/or surface reactions (h^{-1}). All SOA was assumed to be in the $PM_{2.5}$ size range.

The filter removal efficiency (η_{filt}) and the deposition rate for SOA (β_{SOA}) were assumed to be the same as indoor $PM_{2.5}$ as mentioned previously in this section. Indoor SOA mass formation yields for the ozonolysis of indoor terpenoids (Y_{terp}) was calculated using two-product model curves plotted as a function of the indoor organic aerosol concentration (Equation (8)) [124].

$$Y = M_{org} \sum_i \left(\frac{\alpha_i K_i}{1 + M_{org} K_i} \right) \quad (8)$$

where M_{org} is organic aerosol mass concentration ($\mu g\ m^{-3}$) and α_i (−) and K_i ($\mu g\ m^{-3}$) are fitting parameters for the two product model, where $\alpha_1 = 0.082$, $K_1 = 1$, $\alpha_2 = 0.86$, and $K_2 = 0.0055$ for d-limonene and $\alpha_1 = 0.14$, $K_1 = 0.26$, $\alpha_2 = 0.14$, and $K_2 = 0.036$ for α-pinene. We assumed that the fraction of indoor $PM_{2.5}$ of outdoor origin $PM_{2.5}$ that is organic was 30% [125] and we assumed that 80% of indoor origin $PM_{2.5}$ was organic [126].

2.4. Automation of simulations

Multiple Python scripts were used to automate the simulation process, which is summarized in Fig. 2 and described as follows. The energy modeling phase involved automated BEopt and EnergyPlus model runs. BEopt provides an open architecture batch simulation framework for the creation of input files, running of simulations, and parsing of output files via Python. BEopt XML files were used to exchange information between the BEopt interface and the modeling framework. The XML file provides a complete description of a single building, with an element for every input found in the BEopt interface. First, 114 BEopt geometry XML files were manually created, which were then manually expanded to create 209 XML files comprising the baseline model home geometries from the NIST model set. These 209 baseline XML files were then modified using Python to replace specific

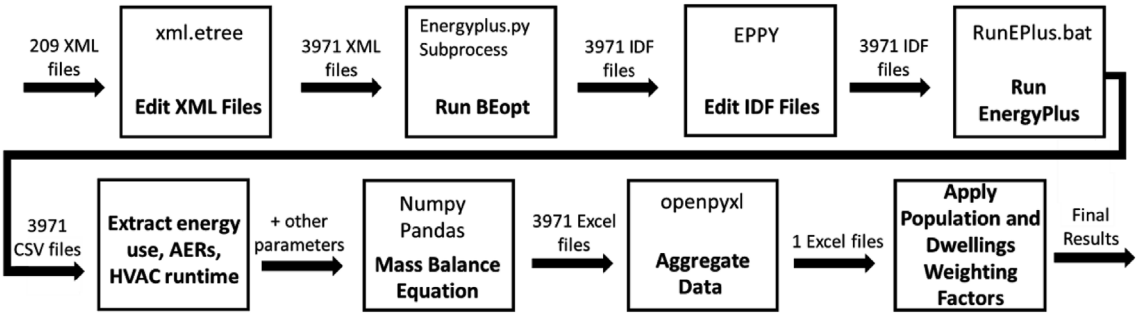

Fig. 2. Model workflow in Python.

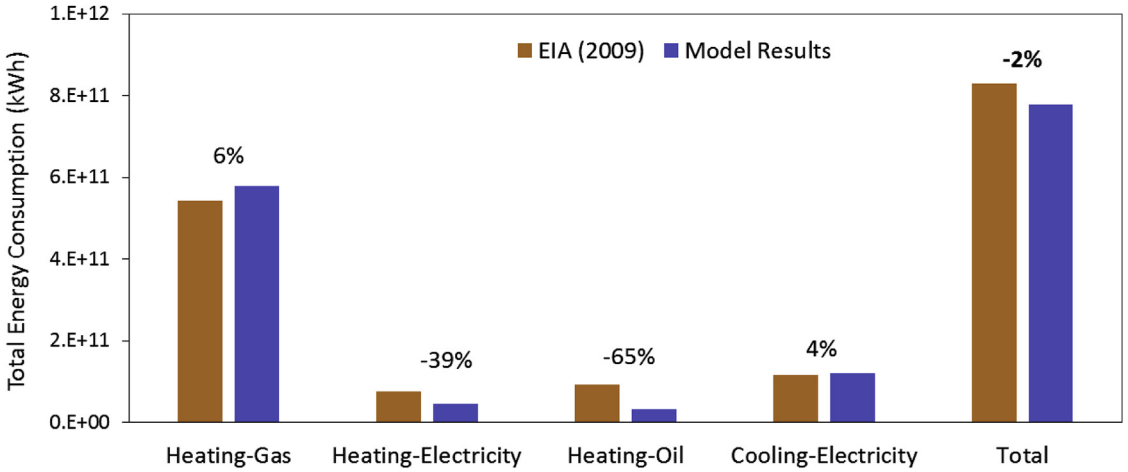

Fig. 3. Total annual residential space conditioning site energy consumption in the U.S. Model results are compared to EIA 2009 RECS data.

construction details with those that vary appropriately by vintage and climate zone to create a total of 3971 XML files (i.e., 3971 individual home models). A package called xml.etree [127] was used to access each baseline element in the XML files, which were then replaced with appropriate inputs for each home and location combination using Python's built-in iterations and the openpyxl package [128] to access to the required data from previously prepared Microsoft Excel files that contained building-specific inputs (i.e., from SI Appendix B).

Next, in order to generate EnergyPlus simulation input files (.IDF) for each home model, the simulation engine's Python script was called with the appropriate XML file provided as an argument. Each IDF file was then edited using eppy.modeleditor [129] to realistically size heating and cooling equipment for each vintage and location as described in section 2.2. Finally, EnergyPlus simulations were automatically run for each home in each location using RunEPlus.bat, a batch procedure file provided with EnergyPlus. The entire energy simulation workflow process, from running the first python script to simulating 3971 EnergyPlus files, took just under two days on a 3.4 GHzPC with 16 GB RAM.

Next, another Python script was used to gather hourly outputs from the EnergyPlus output files, including hourly heating and cooling energy consumption, modeled air change rates (ACRs) through infiltration and natural ventilation separately, and central HVAC system runtimes. Next, some of these outputs (i.e., ACRs and HVAC system runtimes) were used as inputs for the dynamic indoor mass balance models in Equations (5)–(7). Pandas [130] and Numpy [131] Python packages were used to solve the discretized dynamic mass balance equations simultaneously using a forward-marching explicit scheme. Finally, energy and IAQ model results for each of the 3971 unique homes were aggregated into Excel spreadsheet files using openpyxl and were multiplied by population-weighting factors to obtain reasonably realistic nationally representative results for annual HVAC energy use and indoor pollutant concentrations. The IAQ modeling procedure took approximately 5 days on a 3.4 GHz PC with 16 GB RAM; thus, the total simulation time from start to finish was ~7 days. Hourly outputs from the 3971 homes in the REIAQ model set are made available freely online at http://built-envi.com/reiaq/.

2.5. Predicting chronic health impacts

Once population weighted annual average indoor concentrations of the modeled pollutants were calculated, the results were used to estimate the chronic health impacts of residential inhalation exposure to these pollutants using a disability-adjusted life-years (DALYs) approach following the method developed by Logue et al. (2012) [60]. The goal was to recreate nationally representative DALYs associated with chronic exposure to the same pollutants of concern in Logue et al. based on our model results. Methods are described in full in the SI (Appendix E).

3. Results and discussion

3.1. Annual space conditioning energy consumption

Fig. F.1 (Appendix F in the SI) shows estimates of the dwelling-weighted annual space conditioning site energy consumption (including heating, cooling, fan, and hydronic pump energy) aggregated across all home models in each of the 19 cities. The dwelling-weighting multipliers account for the number of homes assumed to be located in each model location. The data are split by vintage (i.e., before 1940, 1940–1969, 1970–1989, and 1990 or after) and by type of HVAC system (i.e., central forced air heating and/or cooling and no central air). As expected, total residential space conditioning energy consumption was estimated to be highest in those cities with both the highest heating degree days and the largest numbers of dwellings (e.g., highest in Chicago, IL, New York, NY, and Washington, DC).

The dwelling-weighted site energy consumption results were also used to estimate the total annual space conditioning energy consumption for the U.S. residential building stock by scaling individual model results by the dwelling-weighting factors for homes in each location. Model results are compared to estimates of end energy usage from the 2009 U.S. EIA Residential Energy Consumption Survey (RECS) [132] in Fig. 3, split by heating and cooling fuel (i.e., heating by electricity, gas, and fuel oil, and cooling by electricity). The total annual space conditioning energy consumption for the entire U.S. residential building stock was estimated in the model set to be $\sim 7.78 \times 10^{11}$ kWh, which was only ~2% lower than the estimate of $\sim 8.30 \times 10^{11}$ kWh made in the 2009 RECS. The largest component of total space conditioning energy use was heating by natural gas, which the model set over-predicted by ~6% relative to the RECS data (5.78×10^{11} kWh compared to 5.43×10^{11} kWh). The next largest component of total space conditioning energy use was cooling by electricity, which the model set over-predicted by just ~4% relative to EIA RECS data (i.e., 1.22×10^{11} kWh compared to 1.17×10^{11} kWh).

Model results for the two smaller contributors to overall space conditioning energy use (i.e., heating by electricity and heating by fuel oil) were substantially lower than EIA RECS data: ~39% lower for electric heating and ~65% lower for fuel oil heating. The reason for these discrepancies is that, as mentioned in Section 2.1.2, the type of heating fuel and system assumed for each modeled home was chosen based only on the most commonly used fuel type in each region (based on information in the RECS survey) in order to limit the number of

Table 5
Annual averages (± standard deviations) of the estimated hourly average air change rates (ACRs) and HVAC runtime fractions.

Year of construction	Mean (standard deviation)			
	Infiltration h^{-1}	Natural ventilation h^{-1}	Total h^{-1}	HVAC runtime %
BEFORE 1940	0.67 (± 0.27)	0.22 (± 0.15)	0.88 (± 0.32)	14.2 (± 4.4)
1940–1969	0.54 (± 0.21)	0.19 (± 0.14)	0.73 (± 0.27)	15.4 (± 5.0)
1970–1989	0.37 (± 0.13)	0.20 (± 0.14)	0.58 (± 0.21)	15.6 (± 5.6)
AFTER 1990	0.24 (± 0.06)	0.16 (± 0.08)	0.40 (± 0.11)	15.8 (± 5.4)

model homes to a manageable number for simulation purposes. Thus, very few homes were modeled with electric or fuel oil based heating, and homes heated with gas were somewhat over sampled. However, this combination of over sampling and under sampling, which led to slight over predictions in gas heating energy and large under-predictions in fuel oil and electric heating energy (the latter of which occurring in a much smaller number of homes than the former), nearly balance out with reasonably accurate electric cooling energy estimates to yield estimates of total annual space conditioning energy use that are very close to the EIA RECS data. Therefore, these results suggest that the REIAQ modeling approach can indeed be used to simulate total annual space conditioning energy consumption across the entire U.S. residential building stock with reasonably accuracy.

3.2. Air change rates and HVAC system runtimes

Annual averages (± standard deviations) of the modeled hourly average air change rates (which include flows through infiltration and natural ventilation separately as well as combined for the total ACR) and HVAC runtime fractions from the 3971 model home simulations are shown in Table 5. Results demonstrate that, as expected, older homes had higher annual average infiltration and total ACRs than newer homes, while natural ventilation ACRs were similar across all vintages. The annual average infiltration and total ACRs ranged from ~0.24 h^{-1} and ~0.4 h^{-1} in the newest homes, respectively, to ~0.67 h^{-1} and ~0.88 h^{-1} in the oldest homes. For comparison, Persily et al. (2010) used the same base model set to estimate infiltration ACRs using CONTAM and reported median infiltration ACRs for the same four home vintages to be 0.58 h^{-1}, 0.54 h^{-1}, 0.36 h^{-1}, and 0.26 h^{-1} for homes built before 1940, between 1940 and 1969, between 1970 and 1989, and 1990 or after, respectively, which are very similar to our model results with values of 0.67 h^{-1}, 0.54 h^{-1}, 0.37 h^{-1}, and 0.24 h^{-1} for the same intervals of year of construction, respectively. Modeled annual average HVAC runtimes were similar across all vintages, averaging approximately 15%. Although we are not aware of large national data sets to which we can compare our runtime estimates, most previous studies of residences in the U.S. (mostly focused in cooling-dominated climates) have reported average fractional HVAC runtimes of approximately 20–25% [24,133].

3.3. Modeled indoor pollutant concentrations

Fig. 4 shows distributions of the resulting annual mean indoor concentrations of all modeled pollutants, infiltration factors for $PM_{2.5}$, UFP, NO_2, and O_3 of outdoor origin, and indoor-outdoor (I/O) ratios for $PM_{2.5}$, UFP, and NO_2 modeled for all 3971 homes. The resulting distributions are also compared to distributions of the average values of the same parameters reported in a large number of field studies primarily in the U.S. and Canada, as described in an extensive literature review in the SI (Appendix G, H, and I for indoor concentrations, infiltration factors, and I/O ratios, respectively). Although the experimental data from the literature review do not necessarily form a nationally representative sample, the intent of the comparison is to demonstrate the likely reasonableness of our model results.

The modeled annual average hourly indoor $PM_{2.5}$ concentrations ranged from 4.6 to 21.6 μg/m^3 with a median value of 11.2 μg/m^3 across all 3971 home models. A review of 19 field studies involving over 690 homes in the U.S. shows a range of average indoor $PM_{2.5}$ concentrations of 5.8–20.3 μg/m^3 with a median value of 13.9 μg/m^3. The median I/O $PM_{2.5}$ concentration ratio from the modeling results and field studies were ~1.1 and ~1.0, respectively. The median $PM_{2.5}$ infiltration factor was ~0.46 in the model results and ~0.6 in the field studies, with ranges of 0.22–0.70 and 0.43–0.74, respectively. While these comparisons suggest the model results are reasonably close to data from field studies, some potential sources for discrepancies include differences in air change rates and the fact that we considered cooking to be the only indoor source of $PM_{2.5}$. While the latter assumption ignores other indoor sources, the assumption of cooking occurring daily for 1 h serves as a likely overestimation of cooking sources that reasonably accounts for other indoor $PM_{2.5}$ sources without assigning other discrete emission events. This simplification does not appear to adversely affect the reasonableness of the model outcomes.

The annual average SOA concentration resulting from the modeled oxidative reactions with ROGs was estimated to be less than 0.1 μg/m^3 in this study, contributing less than 1% to the total indoor $PM_{2.5}$ concentration (with a maximum value of ~3%). For comparison to the literature, Ji and Zhao (2015) [134] estimated the average SOA fraction of indoor $PM_{2.5}$ in China to be ~0.4% with the maximum contribution of ~3%, while Waring (2014) [51] estimated a geometric mean SOA fraction of indoor $PM_{2.5}$ from the RIOPA study data of ~6%. Discrepancies between this work and Waring (2014) most likely stem from our reliance on median indoor ROG emission rates rather than using distributions that would account for a wider range in SOA formation in homes.

Modeled annual average indoor UFP concentrations ranged from ~3×10^3 to ~26×10^3 #/cm^3 with a median of ~11×10^3 #/cm^3, which is similar to the median indoor UFP concentration (~13×10^3 #/cm^3) from four field studies of approximately 90 homes. The median UFP infiltration factors from the modeling and field studies were ~0.20 and ~0.21, respectively, and the median I/O UFP ratios were ~0.9 in both the modeling and field studies. These close similarities are likely due in part to the assumption for cooking activities being the only UFP sources being more realistic than for $PM_{2.5}$, as recent studies have shown that cooking is often the dominant UFP source in both magnitude and frequency of emissions [4].

The NO_2 concentration results were separated by the fuel type used in household stoves (gas or electric) to compare to the literature values. For homes with gas stoves, the modeled annual average indoor NO_2 concentration ranged from 4.9 to 31.7 ppb with a median of 18 ppb, while the median indoor NO_2 concentration from six field studies of more than 800 homes with gas stoves was 24 ppb. For the homes with electric stoves, the modeled annual average indoor NO_2 concentration ranged from 0.9 to 18 ppb with a median of 7 ppb, which was reasonably similar to the median indoor NO_2 concentration from six field studies of nearly 300 homes with electric stoves (which was also 7 ppb). Additionally, the annual average I/O NO_2 concentration ratio for the modeled homes with gas and electric stoves ranged from 0.5 to 4.1 and 0.2–0.8 with median values of 1.4 and 0.5, respectively. The median I/

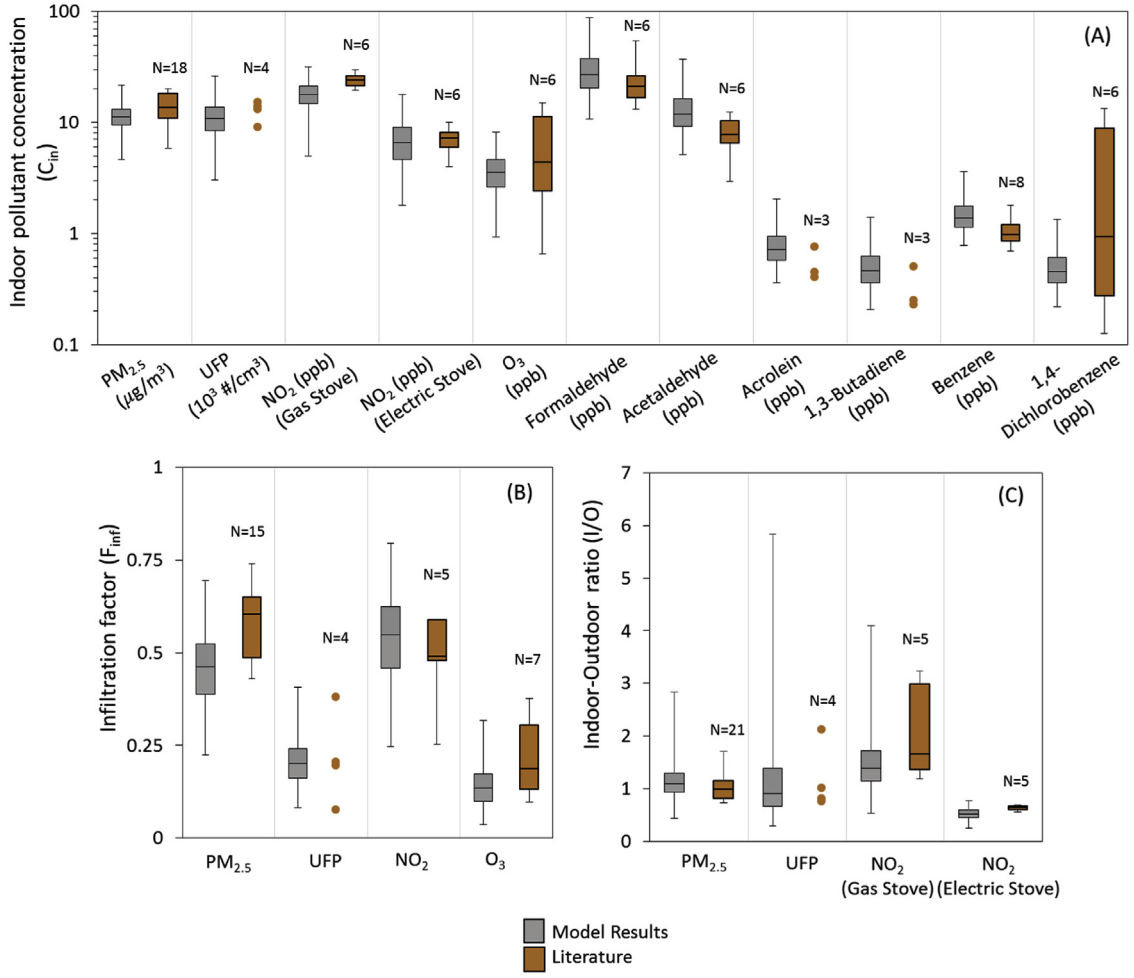

Fig. 4. Annual hourly averages of (A) indoor concentrations of all modeled pollutants (on a log scale), (B) infiltration factors (F_{inf}) for $PM_{2.5}$, UFP, NO_2, and O_3, and (C) I/O ratios for $PM_{2.5}$, UFP, and NO_2 (split by homes with gas and electric stoves) for the 3971 model homes compared to values reported in an extensive literature review for each parameter. The top and bottom of the boxes represent the 25th and 75th percentiles and the end of the whiskers represent the minimum and maximum values. N indicates the number of the studies that were used in the comparison to field measurements in the literature.

O ratios from five field studies of over 800 homes with gas stoves and 450 homes with electric stoves were 1.9 and 0.6, respectively.

Modeled annual average indoor O_3 concentrations ranged from 1 to 8 ppb with a median of 4 ppb. Results from the literature review were similar; the median indoor O_3 concentration from six studies of over 600 homes was also 4 ppb. Modeled results for O_3 infiltration factors ranged from 0.04 to 0.32 with a median of 0.14 and were fairly similar to the values reported in the literature with a range of 0.1–0.38 and a median of 0.19. Finally, the median annual average modeled indoor concentrations of aldehydes and VOCs were 27, 12, 0.7, 0.5, 1.4, and 0.5 for formaldehyde, acetaldehyde, acrolein, 1,3-butadiene, benzene, and 1,4-dichlorobenzene, respectively. The medians and ranges of modeled results were all similar to those reported in field studies in the SI (Appendix G). Combined, these data clearly demonstrate that the model set is capable of reproducing realistic indoor concentrations of a number of pollutants of both indoor and outdoor origin.

3.4. Population weighted annual average indoor pollutant concentrations

Fig. 5 shows the population weighted annual average indoor concentrations of each pollutant modeled in this study calculated by weighting the concentration results from the 3971 individual homes by the population weighting factors for each home in each location. The same population weighted average concentrations are also shown by location in the SI (Appendix J). Although not shown here, population weighted annual average indoor $PM_{2.5}$ concentrations ranged from ~10.5 μg/m³ in the oldest homes (with individual homes ranging from 5.1 to 18.1 μg/m³) to ~7.3 μg/m³ in the newest homes (with individual homes ranging from 4.6 to 21.6 μg/m³). Modeled population weighted annual average $PM_{2.5}$ concentrations of indoor origin were higher in newer homes as a result of lower air change rates combined with assumed constant indoor source strengths, ranging from 1.7 to 9.7 μg/m³, 2.4–11 μg/m³, 2.1–13.1 μg/m³, and 2.4–15.8 μg/m³ for homes built before 1940, 1940–1969, 1970–1989, and after 1990, respectively. Conversely, modeled annual average $PM_{2.5}$ concentrations of outdoor origin were lower in newer homes as a result of lower air change rates. Population weighted annual average indoor UFP concentrations of indoor and outdoor origin followed similar patterns as the $PM_{2.5}$ concentrations, with newer homes having a higher concentration of UFPs of indoor origin and lower concentrations of UFPs of outdoor origin.

Population weighted annual average indoor and outdoor generated NO_2 across the modeled residences ranged from 4.9 to 31.7 ppb for homes with gas stoves and from 1.8 to 18.0 ppb for homes with electric stoves. Because the only source of O_3 was ambient air, population weighted annual average indoor O_3 concentrations were ~50% lower in newer/tighter homes compared to older/leakier homes (i.e., ~4.8 compared to ~2.2 ppb). Finally, the highest population weighted annual average aldehyde and VOC concentrations were 30.9 ppb for formaldehyde and 13.5 ppb for acetaldehyde.

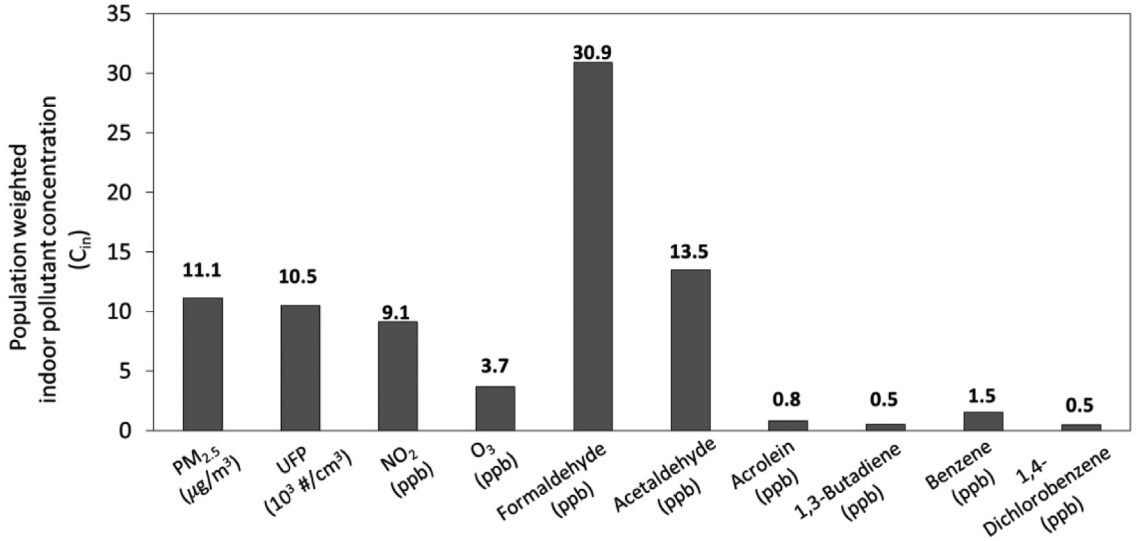

Fig. 5. Population weighted annual average residential indoor concentrations for all modeled pollutants.

3.5. Estimates of DALYs lost due to chronic exposure to residential indoor air pollutants

Fig. 6 shows the estimated number of DALYs lost due to exposure to all pollutants made using the modeled population weighted annual average indoor concentrations from Fig. 5. Estimates of DALYs lost for criteria pollutants (i.e., $PM_{2.5}$, O_3, and NO_2) and aldehydes and VOCs were made using the IND approach and ID approaches in Logue et al. (2012) [60], respectively, as described in the SI (Appendix E). The central estimate of the total DALY burden of chronic pollutant exposures in U.S. residences was approximately 192 DALYs lost per 100,000 persons per year, which is lower than the central estimate made in Logue et al. (2012) [60], likely due in part to our population weighted average concentrations being lower than their representative concentrations used. However, we consider these estimates reasonable based on the extensive comparison between models and measurements in Fig. 4. The largest contributor to total DALYs lost was $PM_{2.5}$ (best estimate of 111 per 100,000 persons per year), followed by acrolein, formaldehyde, O_3, NO_2, and acetaldehyde with 49, 25, 4, 2, and 1 DALYs lost per 100,000 persons per year, respectively.

3.6. Summary of limitations

There are a number of limitations to this work that are worth mentioning and addressing in future versions of the model set. For one, the model set is already out of date in terms of its representativeness for the U.S. building stock. The most immediate need for improvement is to update the model set for homes built since approximately 2000, which will be done following the upcoming release of the 2015 RECS data. Second, there are a number of technical limitations that could be improved. For example, BEopt uses the LBL infiltration model to predict airflows through both infiltration and natural ventilation through window openings. However, to our knowledge, the LBL infiltration model has not been validated for natural ventilation flows. Future improvements could incorporate, at a minimum, the LBLX model to improve the accuracy of natural ventilation modeling [135,136]. Alternatively, the single-zone indirect co-simulation approach could be extended to a multi-zone true co-simulation approach to more accurately predict airflows and contaminant concentrations, for example by integrating CONTAM with EnergyPlus [82].

Other model limitations include our assumptions for constant and ‘typical’ emission rates in each modeled home. Future work should incorporate statistical distributions of indoor emission sources (including distributions of the timing of intermittent sources) to more realistically represent the wide variation in indoor concentrations that have been observed in many field studies [2,63]. Moreover, future work could link whole-house VOC and aldehyde emission rates to factors such as varying indoor air and/or surface temperature and relative humidity as data become available [110,111]. Finally, for the DALY-based chronic health outcome estimation approach, we used unmodified concentration-response function effect estimates from the ambient air quality literature, as did Logue at al. (2012) [60], although it would be more appropriate to modify effect estimates to account for the underlying exposures to pollutants of ambient origin in the various microenvironments in which people spend most of their time [137].

4. Conclusions

A set of nationally representative combined building energy and indoor air mass balance models for the U.S. residential building stock was developed to predict annual space conditioning energy consumption and population weighted average concentrations of several pollutants of both indoor and outdoor origin. The residential energy and indoor air quality (REIAQ) model set was able to predict total annual space conditioning energy consumption for the U.S. residential building stock within ~2% of the 2009 EIA RECS data. Moreover, modeled indoor concentrations, infiltration factors, and indoor/outdoor ratios of several pollutants including $PM_{2.5}$, UFPs, NO_2, O_3, and several VOCs and aldehydes were well within the ranges observed in an extensive review of existing residential field studies in North America. These data were also used to estimate the chronic health burden of residential indoor exposures to be ~192 DALYs lost per person per year. The utility of this model set is that it can be used to investigate the influence of a variety of parameters such as climate zone, ventilation strategy, air infiltration, HVAC system runtimes, and emission sources on both building energy use and indoor air quality across the U.S. residential building stock.

Acknowledgments

This work was supported by the U.S. Environmental Protection Agency under Assistance Agreement No. #83575001 awarded to Illinois Institute of Technology. It has not been formally reviewed by EPA. The views expressed in this document are solely those of the authors and do not necessarily reflect those of the Agency. EPA does not endorse any products or commercial services mentioned in this

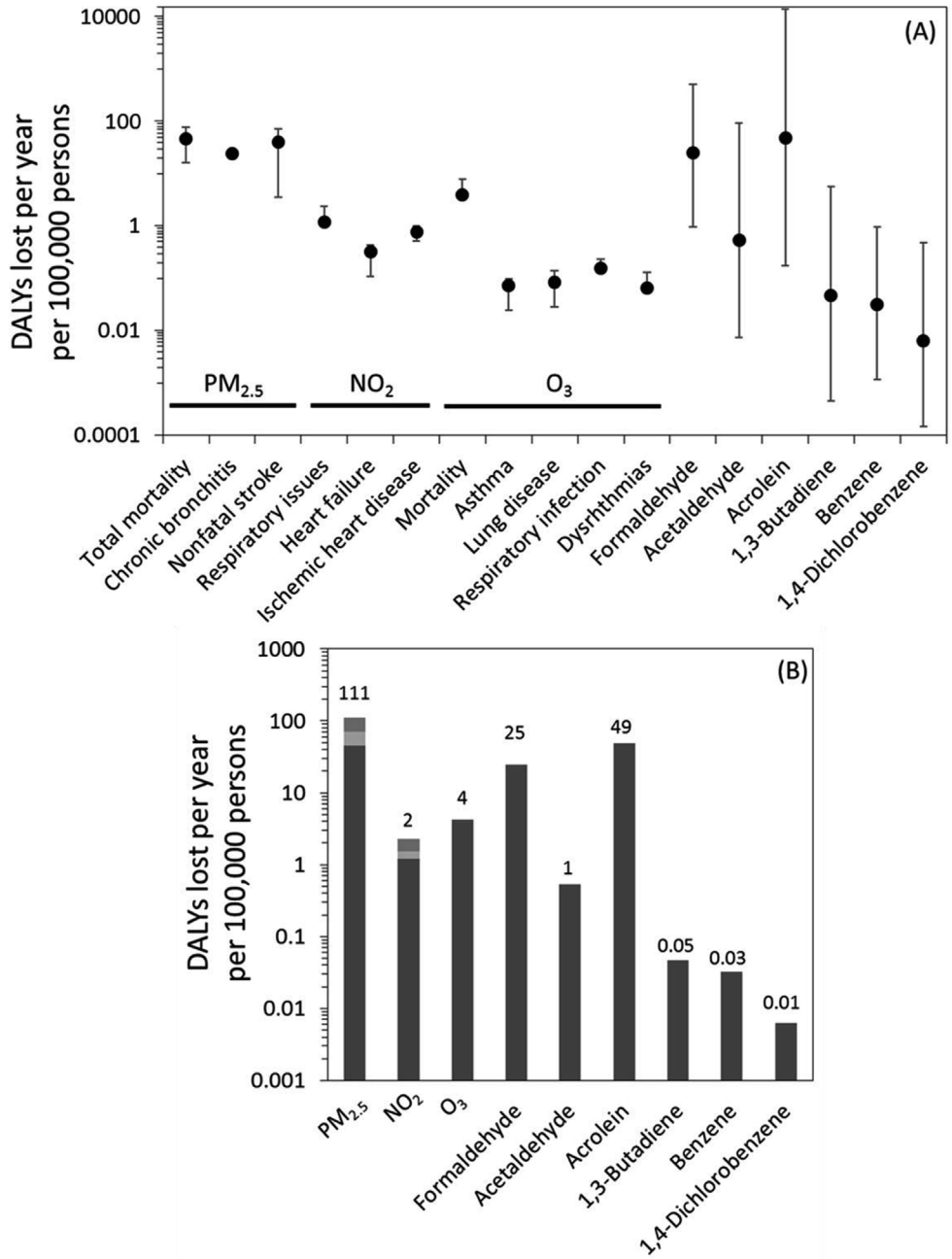

Fig. 6. Best estimates of annual DALYs lost per 100,000 persons using the IND and ID approaches from Logue et al. (2012) [60]. The dots in (a) indicate the central estimate of the DALYs lost and the whiskers show the 95% CI bounds. In (b) the light gray shades for $PM_{2.5}$, NO_2, and O_3 show the various contributions to total DALYs lost from (a).

publication.

Appendix A. Supplementary data

Supplementary data related to this article can be found at http://dx.doi.org/10.1016/j.buildenv.2018.03.047.

References

[1] N.E. Klepeis, W.C. Nelson, W.R. Ott, J.P. Robinson, A.M. Tsang, P. Switzer, et al., The National Human Activity Pattern Survey (NHAPS): a resource for assessing exposure to environmental pollutants, J. Expo. Anal. Environ. Epidemiol. 11 (3) (2001) 231–252.

[2] S.N. Sax, D.H. Bennett, S.N. Chillrud, P.L. Kinney, J.D. Spengler, Differences in source emission rates of volatile organic compounds in inner-city residences of New York City and Los Angeles, J. Expo. Anal. Environ. Epidemiol. 14 (2004) S95–S109.

[3] C.J. Weschler, Ozone's impact on public health: contributions from indoor exposures to ozone and products of ozone-initiated chemistry, Environ. Health Perspect. 114 (10) (2006) 1489–1496.

[4] L. Wallace, W. Ott, Personal exposure to ultrafine particles, J. Expo. Sci. Environ. Epidemiol. 21 (1) (2011) 20–30.

[5] J.M. Logue, T.E. McKone, M.H. Sherman, B.C. Singer, Hazard assessment of chemical air contaminants measured in residences, Indoor Air 21 (2011) 92–109.

[6] K. Sexton, R. Letz, J.D. Spengler, Estimating human exposure to nitrogen dioxide: an indoor/outdoor modeling approach, Environ. Res. 32 (1) (1983) 151–166.

[7] K. Sirén, The protection ability of the building shell against sudden outdoor air contamination, Build. Environ. 28 (3) (1993) 255–269.

[8] T.L. Thatcher, D.W. Layton, Deposition, resuspension, and penetration of particles within a residence, Atmos. Environ. 29 (13) (1995) 1487–1497.

[9] L. Wallace, Indoor particles: a review, J. Air Waste Manag. Assoc. 46 (2) (1996) 98–126.

[10] B.P. Leaderer, L. Naeher, T. Jankun, K. Balenger, T.R. Holford, C. Toth, et al., Indoor, outdoor, and regional summer and winter concentrations of PM10, PM2.5, SO4(2)-, H+, NH4+, NO3-, NH3, and nitrous acid in homes with and without

kerosene space heaters, Environ. Health Perspect. 107 (3) (1999) 223–231.
[11] T.L. Thatcher, M.M. Lunden, K.L. Revzan, R.G. Sextro, N.J. Brown, A concentration rebound method for measuring particle penetration and deposition in the indoor environment, Aerosol. Sci. Technol. 37 (11) (2003) 847–864.
[12] R. Williams, J. Suggs, A. Rea, L. Sheldon, C. Rodes, J. Thornburg, The Research Triangle Park particulate matter panel study: modeling ambient source contribution to personal and residential PM mass concentrations, Atmos. Environ. 37 (38) (2003) 5365–5378.
[13] Q.Y. Meng, B.J. Turpin, L. Korn, C.P. Weisel, M. Morandi, S. Colome, et al., Influence of ambient (outdoor) sources on residential indoor and personal PM2.5 concentrations: analyses of RIOPA data, J. Expo. Anal. Environ. Epidemiol. 15 (1) (2005) 17–28.
[14] D. Rim, L. Wallace, A. Persily, Infiltration of outdoor ultrafine particles into a test house, Environ. Sci. Technol. 44 (15) (2010) 5908–5913.
[15] C. Chen, B. Zhao, Review of relationship between indoor and outdoor particles: I/O ratio, infiltration factor and penetration factor, Atmos. Environ. 45 (2) (2011) 275–288.
[16] H. Zhao, B. Stephens, A method to measure the ozone penetration factor in residences under infiltration conditions: application in a multifamily apartment unit, Indoor Air 26 (4) (2016) 571–581.
[17] H. Zhao, B. Stephens, Using portable particle sizing instrumentation to rapidly measure the penetration of fine and ultrafine particles in unoccupied residences, Indoor Air 27 (1) (2017) 218–229.
[18] B. Stephens, Building design and operational choices that impact indoor exposures to outdoor particulate matter inside residences, Sci. Technol. Built Environ. 21 (1) (2015) 3–13.
[19] B. Stephens, J.A. Siegel, Penetration of ambient submicron particles into single-family residences and associations with building characteristics, Indoor Air 22 (6) (2012) 501–513.
[20] B. Stephens, E.T. Gall, J.A. Siegel, Measuring the penetration of ambient ozone into residential buildings, Environ. Sci. Technol. 46 (2) (2012) 929–936.
[21] C. Chen, B. Zhao, C.J. Weschler, Assessing the influence of indoor exposure to "outdoor ozone" on the relationship between ozone and short-term mortality in U.S. Communities, Environ. Health Perspect. 120 (2) (2012) 235–240.
[22] C. Chen, B. Zhao, C.J. Weschler, Indoor exposure to "outdoor PM10.", Epidemiology 23 (6) (2012) 870–878.
[23] M. MacNeill, L. Wallace, J. Kearney, R.W. Allen, K. Van Ryswyk, S. Judek, et al., Factors influencing variability in the infiltration of PM2.5 mass and its components, Atmos. Environ. 61 (2012) 518–532.
[24] Z. El Orch, B. Stephens, M.S. Waring, Predictions and determinants of size-resolved particle infiltration factors in single-family homes in the U.S. Build. Environ. 74 (2014) 106–118.
[25] J. Kearney, L. Wallace, M. MacNeill, M.-E. Héroux, W. Kindzierski, A. Wheeler, Residential infiltration of fine and ultrafine particles in Edmonton, Atmos. Environ. 94 (2014) 793–805.
[26] M.M. Lunden, T.L. Thatcher, S.V. Hering, N.J. Brown, Use of time- and chemically resolved particulate data to characterize the infiltration of outdoor PM2.5 into a residence in the san joaquin valley, Environ. Sci. Technol. 37 (20) (2003) 4724–4732.
[27] R. Allen, T. Larson, L. Sheppard, L. Wallace, L.-J.S. Liu, Use of real-time light scattering data to estimate the contribution of infiltrated and indoor-generated particles to indoor air, Environ. Sci. Technol. 37 (16) (2003) 3484–3492.
[28] R.W. Allen, S.D. Adar, E. Avol, M. Cohen, C.L. Curl, T. Larson, et al., Modeling the residential infiltration of outdoor PM2.5 in the multi-ethnic study of atherosclerosis and air pollution (MESA air), Environ. Health Perspect. 120 (6) (2012) 824–830.
[29] C.M. Long, H.H. Suh, P.J. Catalano, P. Koutrakis, Using time- and size-resolved particulate data to quantify indoor penetration and deposition behavior, Environ. Sci. Technol. 35 (10) (2001) 2089–2099.
[30] N. Hodas, Q. Meng, M.M. Lunden, D.Q. Rich, H. Özkaynak, L.K. Baxter, et al., Variability in the fraction of ambient fine particulate matter found indoors and observed heterogeneity in health effect estimates, J. Expo. Sci. Environ. Epidemiol. 22 (5) (2012) 448–454.
[31] N. Hodas, B.J. Turpin, Shifts in the gas-particle partitioning of ambient organics with transport into the indoor environment, Aerosol. Sci. Technol. (2013) 131207050823004.
[32] L.K. Baxter, J. Burke, M. Lunden, B.J. Turpin, D.Q. Rich, K. Thevenet-Morrison, et al., Influence of human activity patterns, particle composition, and residential air exchange rates on modeled distributions of PM2.5 exposure compared with central-site monitoring data, J. Expo. Sci. Environ. Epidemiol. 23 (2013) 241–247.
[33] L.A. Wallace, E. Pellizzari, B. Leaderer, H. Zelon, L. Sheldon, Emissions of volatile organic compounds from building materials and consumer products, Atmos. Environ. 21 (2) (1967) 385–393 1987.
[34] P. Wolkoff, Impact of air velocity, temperature, humidity, and air on long-term voc emissions from building products, Atmos. Environ. 32 (14–15) (1998) 2659–2668.
[35] W.W. Nazaroff, C.J. Weschler, Cleaning products and air fresheners: exposure to primary and secondary air pollutants, Atmos. Environ. 38 (18) (2004) 2841–2865.
[36] B.C. Singer, H. Destaillats, A.T. Hodgson, W.W. Nazaroff, Cleaning products and air fresheners: emissions and resulting concentrations of glycol ethers and terpenoids, Indoor Air 16 (3) (2006) 179–191.
[37] A.C. Steinemann, I.C. MacGregor, S.M. Gordon, L.G. Gallagher, A.L. Davis, D.S. Ribeiro, et al., Fragranced consumer products: chemicals emitted, ingredients unlisted, Environ. Impact Assess. Rev. 31 (3) (2011) 328–333.
[38] C.J. Weschler, W.W. Nazaroff, Semivolatile organic compounds in indoor environments, Atmos. Environ. 42 (40) (2008) 9018–9040.
[39] L.A. Wallace, S.J. Emmerich, C. Howard-Reed, Source strengths of ultrafine and fine particles due to cooking with a gas stove, Environ. Sci. Technol. 38 (8) (2004) 2304–2311.
[40] A. Afshari, U. Matson, L.E. Ekberg, Characterization of indoor sources of fine and ultrafine particles: a study conducted in a full-scale chamber, Indoor Air 15 (2) (2005) 141–150.
[41] W.R. Ott, H.C. Siegmann, Using multiple continuous fine particle monitors to characterize tobacco, incense, candle, cooking, wood burning, and vehicular sources in indoor, outdoor, and in-transit settings, Atmos. Environ. 40 (5) (2006) 821–843.
[42] C. He, L. Morawska, L. Taplin, Particle emission characteristics of office printers, Environ. Sci. Technol. 41 (17) (2007) 6039–6045.
[43] A.R. Ferro, R.J. Kopperud, L.M. Hildemann, Source strengths for indoor human activities that resuspend particulate matter, Environ. Sci. Technol. 38 (6) (2004) 1759–1764.
[44] J. Qian, A.R. Ferro, Resuspension of dust particles in a chamber and associated environmental factors, Aerosol. Sci. Technol. 42 (7) (2008) 566–578.
[45] C.J. Weschler, A.T. Hodgson, J.D. Wooley, Indoor chemistry: ozone, volatile organic compounds, and carpets, Environ. Sci. Technol. 26 (12) (1992) 2371–2377.
[46] C.J. Weschler, H.C. Shields, Indoor ozone/terpene reactions as a source of indoor particles, Atmos. Environ. 33 (15) (1999) 2301–2312.
[47] G. Sarwar, R. Corsi, D. Allen, C. Weschler, The significance of secondary organic aerosol formation and growth in buildings: experimental and computational evidence, Atmos. Environ. 37 (9–10) (2003) 1365–1381.
[48] H. Destaillats, M.M. Lunden, B.C. Singer, B.K. Coleman, A.T. Hodgson, C.J. Weschler, et al., Indoor secondary pollutants from household product emissions in the presence of Ozone: a bench-scale chamber study, Environ. Sci. Technol. 40 (14) (2006) 4421–4428.
[49] J.E. Ham, J.R. Wells, Surface chemistry of a pine-oil cleaner and other terpene mixtures with ozone on vinyl flooring tiles, Chemosphere 83 (3) (2011) 327–333.
[50] M.S. Waring, J.R. Wells, J.A. Siegel, Secondary organic aerosol formation from ozone reactions with single terpenoids and terpenoid mixtures, Atmos. Environ. 45 (25) (2011) 4235–4242.
[51] M.S. Waring, Secondary organic aerosol in residences: predicting its fraction of fine particle mass and determinants of formation strength, Indoor Air 24 (2014) 376–389.
[52] C.J. Weschler, Ozone in indoor environments: concentration and chemistry, Indoor Air 10 (4) (2000) 269–288.
[53] A. Wisthaler, C.J. Weschler, Reactions of ozone with human skin lipids: sources of carbonyls, dicarbonyls, and hydroxycarbonyls in indoor air, Proc. Natl. Acad. Sci. Unit. States Am. 107 (15) (2010) 6568–6575.
[54] M.S. Waring, J.A. Siegel, Indoor secondary organic aerosol formation initiated from reactions between ozone and surface-sorbed d -limonene, Environ. Sci. Technol. (2013) 130531095809003.
[55] C. Wang, M.S. Waring, Secondary organic aerosol formation initiated from reactions between ozone and surface-sorbed squalene, Atmos. Environ. 84 (2014) 222–229.
[56] J.M. Logue, T.E. McKone, M.H. Sherman, B.C. Singer, Hazard assessment of chemical air contaminants measured in residences, Indoor Air 21 (2011) 92–109.
[57] S.K. Brown, Chamber assessment of formaldehyde and VOC emissions from wood-based panels, Indoor Air 9 (3) (1999) 209–215.
[58] T.J. Kelly, D.L. Smith, J. Satola, Emission rates of formaldehyde from materials and consumer products found in California homes, Environ. Sci. Technol. 33 (1) (1999) 81–88.
[59] W. Liu, J. Zhang, L. Zhang, B. Turpin, C. Weisel, M. Morandi, et al., Estimating contributions of indoor and outdoor sources to indoor carbonyl concentrations in three urban areas of the United States, Atmos. Environ. 40 (12) (2006) 2202–2214.
[60] J.M. Logue, P.N. Price, M.H. Sherman, B.C. Singer, A method to estimate the chronic health impact of air pollutants in U.S. residences, Environ. Health Perspect. 120 (2) (2012) 216–222.
[61] L.A. Wallace, Comparison of risks from outdoor and indoor exposure to toxic chemicals, Environ. Health Perspect. 95 (1991) 7–13.
[62] S.N. Sax, D.H. Bennett, S.N. Chillrud, J. Ross, P.L. Kinney, J.D. Spengler, A cancer risk assessment of inner-city teenagers living in New York city and los angeles, Environ. Health Perspect. 114 (10) (2006) 1558–1566.
[63] D.E. Hun, J.A. Siegel, M.T. Morandi, T.H. Stock, R.L. Corsi, Cancer risk disparities between hispanic and non-hispanic white populations: the role of exposure to indoor air pollution, Environ. Health Perspect. 117 (12) (2009) 1925–1931.
[64] Table 113 Build. Share US Prim. Energy Consum, Buildings Energy Data Book [Internet], DOE, 2012 Available from: http://buildingsdatabook.eren.doe.gov/TableView.aspx?table=1.1.3.
[65] HUD. American Housing Survey for the United States, Table 1A-4: Selected Equipment and Plumbing [Internet], U.S. Census Bureau, 2007 2007 [cited 2010]. Available from: http://www.census.gov/hhes/www/housing/ahs/ahs07/tab1a-4.pdf.
[66] DOE. Buildings Energy Data Book [Internet]. Table 215 2010 Resid. Energy End-Use Splits. 2011 [cited 2012]. Available from: http://buildingsdatabook.eren.doe.gov/TableView.aspx?table=2.1.6.
[67] ASHRAE, ASHRAE Handbook of Fundamentals: Chapter 16: Ventilation and Infiltration, American Society of Heating, Refrigerating and Air-Conditioning Engineers, 2013.
[68] M. Sherman, N. Matson, Airtightness of U.S. dwellings, Build. Eng. 103 (1) (1997) 717–730.
[69] W. Chan, W. Nazaroff, P. Price, M. Sohn, A. Gadgil, Analyzing a database of residential air leakage in the United States, Atmos. Environ. 39 (19) (2005) 3445–3455.

[70] W.R. Chan, J. Joh, M.H. Sherman, Analysis of air leakage measurements of US houses, Energy Build. 66 (2013) 616–625.
[71] J. Thornburg, D.S. Ensor, C.E. Rodes, P.A. Lawless, L.E. Sparks, R.B. Mosley, Penetration of particles into buildings and associated physical factors. Part I: model development and computer simulations, Aerosol. Sci. Technol. 34 (3) (2001) 284–296.
[72] D.L. MacIntosh, T. Minegishi, M. Kaufman, B.J. Baker, J.G. Allen, J.I. Levy, et al., The benefits of whole-house in-duct air cleaning in reducing exposures to fine particulate matter of outdoor origin: a modeling analysis, J. Expo. Sci. Environ. Epidemiol. 20 (2) (2010) 213–224.
[73] P. Azimi, D. Zhao, B. Stephens, Modeling the impact of residential HVAC filtration on indoor particles of outdoor origin (RP-1691), Sci. Technol. Built Environ. 22 (4) (2016) 431–462.
[74] I.S. Walker, D.J. Dickerhoff, D. Faulkner, W.J.N. Turner, Energy Implications of In-Line Filtration in California, Lawrence Berkeley National Laboratory, Berkeley, CA, 2012 Report No.: LBNL-6143E.
[75] I.S. Walker, M.H. Sherman, Energy implications of meeting ASHRAE standard 62.2, ASHRAE Trans. 114 (2) (2008) 505–516.
[76] T. Fazli, R.Y. Yeap, B. Stephens, Modeling the energy and cost impacts of excess static pressure in central forced-air heating and air-conditioning systems in single-family residences in the U.S, Energy Build. 107 (2015) 243–253.
[77] B. Stephens, A. Novoselac, J.A. Siegel, The effects of filtration on pressure drop and energy consumption in residential HVAC systems, HVAC R Res. 16 (3) (2010) 273–294.
[78] B. Stephens, J.A. Siegel, A. Novoselac, Energy implications of filtration in residential and light-commercial buildings (RP-1299), ASHRAE Trans. 116 (1) (2010) 346–357.
[79] A. Persily, A. Musser, S.J. Emmerich, Modeled infiltration rate distributions for U.S. housing, Indoor Air 20 (6) (2010) 473–485.
[80] A.K. Persily, A. Musser, D. Leber, A Collection of Homes to Represent the U.S. Housing Stock, National Institute of Standards and Technology (NIST), Gaithersburg, MD, 2006 Report No.: NISTIR 7330.
[81] G.N. Walton, W.S. Dols, CONTAM, National Institutes of Standards and Technology, 2008.
[82] W.S. Dols, S.J. Emmerich, B.J. Polidoro, Coupling the multizone airflow and contaminant transport software CONTAM with EnergyPlus using co-simulation, Build. Simul. 9 (4) (2016) 469–479.
[83] J.M. Logue, M.H. Sherman, M.M. Lunden, N.E. Klepeis, R. Williams, C. Croghan, et al., Development and assessment of a physics-based simulation model to investigate residential PM2.5 infiltration across the US housing stock, Build. Environ. 94 (2015) 21–32.
[84] J.M. Logue, N.E. Klepeis, A.B. Lobscheid, B.C. Singer, Pollutant exposures from natural gas cooking burners: a simulation-based assessment for southern California, Environ. Health Perspect. 122 (1) (2014) 43–50.
[85] Software Help | BEopt [Internet]. [cited 2017]. Available from: https://beopt.nrel.gov/softwareHelp.
[86] 1999 [cited 2010], HUD. American Housing Survey for the United States, U.S. Department of Housing and Urban Development, U.S. Department of Commerce, Washington, DC, 1999 Available from: http://www.census.gov/hhes/www/housing/ahs/ahs07/tab1a-4.pdf.
[87] DOE, A Look at Residential Energy Consumption in 1997, DOE/EIA-0632(97) U.S. Department of Energy, Washington, DC, 1999.
[88] M. Sherman, D. Dickerhoff, Airtightness of U.S. dwellings, ASHRAE Trans. 104 (1998).
[89] ASHRAE, ASHRAE Standard 119. Air Leakage Performance for Detached Single-family Residential Buildings, American Society of Heating, Refrigerating and Air-Conditioning Engineers, 2004.
[90] Robert Hendron, Building America Performance Analysis Procedures for Existing Homes, Report No.: No. NREL/TP–550–38238 EERE Publication and Product Library, 2006.
[91] Y.J. Huang, R. Ritschard, J. Bull, S. Byrne, I. Turiel, D. Wilson, et al., Methodology and Assumptions for Evaluating Heating and Cooling Energy Requirements in New Single-family Residential Buildings: Technical Support Document for the Pear (Program for Energy Analysis of Residences) Microcomputer Program [Internet], Lawrence Berkeley Lab., CA (USA), 1987 Available from: http://www.osti.gov/scitech/biblio/6533484.
[92] J. Huang, J. Hanford, F. Yang, Residential Heating and Cooling Loads Component Analysis [Internet], Building Technologies Department, Environmental Energy Technologies Division, Lawrence Berkeley National Laboratory, University of California, 1999 [cited 2015]. Available from: http://simulationresearch.lbl.gov/dirpubs/44636.pdf.
[93] J. Apte, D. Arasteh, Window-Related Energy Consumption in the US Residential and Commercial Building Stock, Lawrence Berkeley Natl. Lab. [Internet], 2008 [cited 2016]; Available from: http://escholarship.org/uc/item/9vx6b6pv.
[94] International Energy Conservation Code, IECC, 2000 Available from: https://law.resource.org/pub/us/code/ibr/icc.iecc.2000.pdf.
[95] B. Ward, J. Steward, J. Jackson, Energy Savings from Honeywell Total Connect Comfort Thermostats, Report prepared for Honeywell International Incorporated Smart Grid Solutions, 2014, https://www.honeywellsmartgrid.com/Resource%20Library/Cadmus%20White%20Paper%20-%20Energy%20Savings%20from%20Honeywell%20Connected%20Thermostats%2013OCT2014_Final.pdf.
[96] B. Stephens, The impacts of duct design on life cycle costs of central residential heating and air-conditioning systems, Energy Build. 82 (2014) 563–579.
[97] J. Proctor, Residential AC filters, ASHRAE J. 48 (October 2012) (2012) 92–93.
[98] J. Proctor, R. Chitwood, B. Wilcox, Efficiency Characteristics and Opportunities for New California Homes, California Energy Commission, 2011 Report No.: CEC-500-2012-062.
[99] J. Proctor, Residential AC filters, ASHRAE J. 48 (October 2012) (2012) 92–93.
[100] D.S. Parker, J.R. Sherwin, R.A. Raustad, D.B. Shirey, Impact of evaporator coil airflow in residential air-conditioning systems, ASHRAE Trans. 103 (1997) 395–405.
[101] DOE, Buildings Energy Data Book [Internet], Table 219 2005 Deliv. Energy End-Uses Aver. Househ. Reg. Million Btu Househ (2012) [cited 2015]. Available from: http://buildingsdatabook.eren.doe.gov/TableView.aspx?table=2.1.9.
[102] N.L. Nagda, M.D. Koontz, R.C. Fortmann, I.H. Billick, Prevalence, use, and effectiveness of range-exhaust fans, Environ. Int. 15 (1) (1989) 615–620.
[103] V. Klug, A. Lobscheid, B. Singer, Cooking appliance use in california homes data collected from a web-based survey, Ernest Orlando Lawrence Berkeley National Laboratory, Berkeley, CA (US), 2011.
[104] E. Wilson, C.E. Metzger, S. Horowitz, R. Hendron, Building America House Simulation Protocols [Internet], National Renewable Energy Laboratory, 2014 2014 [cited 2015]. Available from: https://buildingsfieldtest.nrel.gov/sites/default/files/pdfs/house_simulation_protocols_2014.pdf.
[105] M.H. Sherman, D.T. Grimsrud, Infiltration-pressurization correlation: simplified physical modeling, ASHRAE Trans. 86 (2) (1980) 778–807.
[106] White Box Technologies, Weather Data for Energy Calculations: Historical Data [Internet], White Box Technol. Weather Data, 2015 Available from: http://weather.whiteboxtechnologies.com/wd-hist.
[107] US EPA, Download Detailed AQS Data [Internet], Technol. Transf. Netw. TTN Air Qual. Syst. AQS (2013) [cited 2014]. Available from: http://www.epa.gov/ttn/airs/airsaqs/detaildata/downloadaqsdata.htm.
[108] C.P. Weisel, J (Jim) Zhang, B.J. Turpin, M.T. Morandi, S. Colome, T.H. Stock, et al., Relationship of Indoor, Outdoor and Personal Air (RIOPA) study: study design, methods and quality assurance/control results, J. Expo. Anal. Environ. Epidemiol. 15 (2004) 123–137.
[109] W.R. Chan, J.M. Logue, X. Wu, N.E. Klepeis, W.J. Fisk, F. Noris, et al., Quantifying fine particle emission events from time-resolved measurements: method description and application to 18 California low-income apartments, Indoor Air 28 (1) (2018) 89–101. Available from: http://doi.wiley.com/10.1111/ina.12425.
[110] J. Xiong, W. Wei, S. Huang, Y. Zhang, Association between the emission rate and temperature for chemical pollutants in building materials: general correlation and understanding, Environ. Sci. Technol. (2013) 130709124156006.
[111] C.-C. Lin, K.-P. Yu, P. Zhao, G. Whei-May Lee, Evaluation of impact factors on VOC emissions and concentrations from wooden flooring based on chamber tests, Build. Environ. 44 (3) (2009) 525–533.
[112] C. He, L. Morawska, J. Hitchins, D. Gilbert, Contribution from indoor sources to particle number and mass concentrations in residential houses, Atmos. Environ. 38 (21) (2004) 3405–3415.
[113] G. Buonanno, L. Morawska, L. Stabile, Particle emission factors during cooking activities, Atmos. Environ. 43 (20) (2009) 3235–3242.
[114] D.J. Moschandreas, S.M. Relwani, Field measurements of NO2 gas range-top burner emission rates, Environ. Int. 15 (1) (1989) 489–492.
[115] S.M. Relwani, D.J. Moschandreas, I.H. Billick, Effects of operational factors on pollutant emission rates from residential gas appliances, J. Air Pollut. Contr. Assoc. 36 (11) (1986) 1233–1237.
[116] W.W. Delp, B.C. Singer, Performance assessment of U.S. Residential cooking exhaust hoods, Environ. Sci. Technol. 46 (11) (2012) 6167–6173.
[117] P. Fabian, G. Adamkiewicz, J.I. Levy, Simulating indoor concentrations of NO2 and PM2.5 in multifamily housing for use in health-based intervention modeling: CONTAM simulation of indoor NO2 and PM2.5, Indoor Air 22 (1) (2012) 12–23.
[118] D. Rim, L.A. Wallace, A.K. Persily, Indoor ultrafine particles of outdoor origin: importance of window opening area and fan operation condition, Environ. Sci. Technol. 47 (4) (2013) 1922–1929.
[119] E. Abt, H.H. Suh, P. Catalano, P. Koutrakis, Relative contribution of outdoor and indoor particle sources to indoor concentrations, Environ. Sci. Technol. 34 (17) (2000) 3579–3587.
[120] J. Kearney, L. Wallace, M. MacNeill, X. Xu, K. VanRyswyk, H. You, et al., Residential indoor and outdoor ultrafine particles in Windsor, Ontario, Atmos. Environ. 45 (40) (2011) 7583–7593.
[121] K. Lee, J. Vallarino, T. Dumyahn, H. Ozkaynak, J.D. Spengler, Ozone decay rates in residences, J. Air Waste Manag. Assoc. 49 (10) (1999) 1238–1244.
[122] F. Noris, G. Adamkiewicz, W.W. Delp, T. Hotchi, M. Russell, B.C. Singer, et al., Indoor environmental quality benefits of apartment energy retrofits, Build. Environ. 68 (2013) 170–178.
[123] R. Hecker, K.C. Hofacre, Development of Performance Data for Common Building Air Cleaning Devices, Office of Research and Development/National Homeland Security Research Center Research Triangle Park, NC: U.S. Environmental Protection Agency, 2008 Report No.: EPA/600/R-08/013.
[124] S. Youssefi, M.S. Waring, Predicting secondary organic aerosol formation from terpenoid ozonolysis with varying yields in indoor environments, Indoor Air 22 (5) (2012) 415–426.
[125] A. Polidori, B. Turpin, Q.Y. Meng, J.H. Lee, C. Weisel, M. Morandi, et al., Fine organic particulate matter dominates indoor-generated PM2.5 in RIOPA homes, J. Expo. Sci. Environ. Epidemiol. Tuxedo 16 (4) (2006) 321–331.
[126] S.W. See, R. Balasubramanian, Chemical characteristics of fine particles emitted from different gas cooking methods, Atmos. Environ. 42 (39) (2008) 8852–8862.
[127] 19.7. xml.etree.ElementTree — The ElementTree XML API — Python v2.7.3 documentation [Internet]. [cited 2017]. Available from: https://docs.python.org/2/library/xml.etree.elementtree.html#xml.etree.ElementTree.ElementTree.
[128] Eric Gazoni, Charlie Clark. openpyxl -A Python library to read/write Excel 2010 xlsx/xlsm files [Internet]. [cited 2017]. Available from: https://openpyxl.readthedocs.org/en/latest/.

[129] Philip S, Tran T, Tanjuatco L. eppy: scripting language for E+ [Internet]. [cited 2017]. Available from: https://pypi.python.org/pypi/eppy/0.4.0.
[130] Wes McKinney, Pandas- data structures for statistical computing in Python, Proceedings of the 9th Python in Science Conference, 2010, pp. 51–56.
[131] S. van der Walt, S.C. Colbert, G. Varoquaux, The NumPy array: a structure for efficient numerical computation, Comput. Sci. Eng. 13 (2) (2011) 22–30.
[132] EIA, Buildings Energy Data Book: New Residential Buildings Construction and Companies [Internet], (2009) [cited 2011]. Available from: http://buildingsdatabook.eren.doe.gov/TableView.aspx?table=2.5.8.
[133] K.S. Cetin, A. Novoselac, Single and multi-family residential central all-air HVAC system operational characteristics in cooling-dominated climate, Energy Build. 96 (2015) 210–220.
[134] W. Ji, B. Zhao, Contribution of outdoor-originating particles, indoor-emitted particles and indoor secondary organic aerosol (SOA) to residential indoor PM2.5 concentration: a model-based estimation, Build. Environ. 90 (Supplement C) (2015) 196–205.
[135] M.S. Breen, M. Breen, R.W. Williams, B.D. Schultz, Predicting residential air exchange rates from questionnaires and meteorology: model evaluation in central North Carolina, Environ. Sci. Technol. 44 (24) (2010) 9349–9356.
[136] M.S. Breen, B.D. Schultz, M.D. Sohn, T. Long, J. Langstaff, R. Williams, et al., A review of air exchange rate models for air pollution exposure assessments, J. Expo. Sci. Environ. Epidemiol. [Internet] 24 (2014) 555–563. Available from: http://www.nature.com/doifinder/10.1038/jes.2013.30.
[137] D. Zhao, P. Azimi, B. Stephens, Evaluating the long-term health and economic impacts of central residential air filtration for reducing premature mortality associated with indoor fine particulate matter (PM2.5) of outdoor origin, Int. J. Environ. Res. Publ. Health 12 (7) (2015) 8448–8479.